

# Early-life stress induces persistent astrocyte dysfunction associated with fear generalisation

Mathias Guayasamin<sup>1,2†</sup>, Lewis R Depaauw-Holt<sup>1,2†</sup>, Ifeoluwa I Adedipe<sup>1,2†</sup>, Ossama Ghenissa<sup>1,2</sup>, Juliette Vaugeois<sup>1,2</sup>, Manon Duquenne<sup>1,2</sup>, Benjamin Rogers<sup>1,2</sup>, Jade Latraverse-Arquilla<sup>2</sup>, Sarah Peyrard<sup>2</sup>, Anthony Bosson<sup>2</sup>, Ciaran Murphy-Royal<sup>1,2\*</sup>

<sup>1</sup>Département de Neurosciences, Université de Montréal, Montréal, Canada; <sup>2</sup>Centre de Recherche du Centre Hospitalier de l'Université de Montréal, Montréal, Canada

## eLife Assessment

This **important** article explores the impact of early-life stress (ELS) on adult brain and behaviour. The significance of the **convincing** findings is that they implicate regulation of non-neuronal cells in the development of brain and behavioural dysfunction associated with ELS. With an elegant combination of behavioural models, morphological and functional assessments using immunostaining, electrophysiology, and viral-mediated loss-of-function approaches, the authors report that astrocyte dysfunction plays a role in ELS responses. The work is of interest to a broad behavioural and cellular neuroscience audience.

### \*For correspondence:

ciaran.murphy-royal@umontreal.ca

†These authors contributed equally to this work

**Competing interest:** The authors declare that no competing interests exist.

**Funding:** See page 18

**Preprint posted**

30 May 2024

**Sent for Review**

30 May 2024

**Reviewed preprint posted**

06 August 2024

**Reviewed preprint revised**

15 January 2025

**Version of Record published**

05 February 2025

**Reviewing Editor:** Matthew N Hill, University of Calgary, Canada

© Copyright Guayasamin, Depaauw-Holt, Adedipe *et al.* This article is distributed under the terms of the [Creative Commons Attribution License](https://creativecommons.org/licenses/by/4.0/), which permits unrestricted use and redistribution provided that the original author and source are credited.

**Abstract** Early-life stress can have lifelong consequences, enhancing stress susceptibility and resulting in behavioural and cognitive deficits. While the effects of early-life stress on neuronal function have been well-described, we still know very little about the contribution of non-neuronal brain cells. Investigating the complex interactions between distinct brain cell types is critical to fully understand how cellular changes manifest as behavioural deficits following early-life stress. Here, using male and female mice we report that early-life stress induces anxiety-like behaviour and fear generalisation in an amygdala-dependent learning and memory task. These behavioural changes were associated with impaired synaptic plasticity, increased neural excitability, and astrocyte hypo-function. Genetic perturbation of amygdala astrocyte function by either reducing astrocyte calcium activity or reducing astrocyte network function was sufficient to replicate cellular, synaptic, and fear memory generalisation associated with early-life stress. Our data reveal a role of astrocytes in tuning emotionally salient memory and provide mechanistic links between early-life stress, astrocyte hypo-function, and behavioural deficits.

## Introduction

Both human and rodent studies have provided compelling evidence for the long-lasting effects of adverse early-life experiences, highlighting enhanced susceptibility to subsequent stressors later in life (*Walker et al., 2017; Joëls and Baram, 2009; Lopez and Bagot, 2021; O'Donnell and Meaney, 2020; Meaney, 2001*). Early-life stress (ELS) has widespread effects across the brain and can influence many neural circuits including those involved in threat detection, emotion, cognitive processing, and reward-seeking behaviours (*Peña et al., 2017; Peña et al., 2019; Lesuis et al., 2018; Lesuis et al., 2019*). Research investigating the neurobiology of stress has predominantly focused upon

the effects on neurons and resulting behaviour (Ramkumar et al., 2024; Lupien et al., 2009; Bains et al., 2015; Senst et al., 2016; Wamsteeker Cusulin et al., 2013; Füzési et al., 2016; Daviu et al., 2020; Guadagno et al., 2018b; Guadagno et al., 2021; Guadagno et al., 2018a). We have gleaned tremendous insight into disorders of stress from these studies, yet the links between stress, brain circuits, and behaviour remain tenuous. Within this framework, the contribution of distinct brain cells, including astrocytes, remains largely untested. Glial cells, which comprise approximately half the cell population in the brain, have been shown to directly regulate synaptic transmission and plasticity (Murphy-Royal et al., 2015; Murphy-Royal et al., 2020; Lau et al., 2021; Henneberger et al., 2010; Papouin et al., 2017; Covelo and Araque, 2018; Panatier et al., 2011; Panatier et al., 2006; Matos et al., 2018; Lefton et al., 2024; Guttenplan et al., 2024), thereby influencing many discrete behaviours (Nagai et al., 2021; Wahis et al., 2021; Robin et al., 2018; Martin-Fernandez et al., 2017; Yu et al., 2018; Nagai et al., 2019; Doron et al., 2022; Adamsky et al., 2018; Kol et al., 2020; Mu et al., 2019; Chen et al., 2024). Despite research suggesting important roles for astrocytes in regulating affective states (Wahis et al., 2021; Martin-Fernandez et al., 2017), fear (Martin-Fernandez et al., 2017), reward and addiction behaviours (Doron et al., 2022; Kruyer et al., 2022; Kruyer et al., 2019), whether astrocyte dysfunction prompts stress-induced behavioural impairments remains poorly understood.

First, we characterised whether ELS influenced stress hormone levels across our experimental paradigm from pre-stress until young adulthood. We report that that ELS induces a transient increase in blood glucocorticoids that peaks during late adolescence/young adulthood. Turning to behaviour, this increase in glucocorticoid levels was associated with anxiety-like behaviour in the elevated plus maze.

Next, we set out to determine whether ELS influenced cognitive function using an amygdala-dependent threat discrimination assay. This task was specifically chosen to test the effects of ELS on amygdala function as this brain region is involved with threat detection and associative learning that is acutely sensitive to stress (Guadagno et al., 2018b; Guadagno et al., 2021; Ressler, 2010; Malter Cohen et al., 2013; Roozendaal et al., 2009). We employed an auditory discriminative fear conditioning paradigm that requires synaptic plasticity changes in the lateral amygdala (Kim and Cho, 2017) and found that ELS impairs discriminative fear memory, resulting in fear generalisation. These hormonal and behavioural changes were associated with impaired synaptic plasticity and enhanced excitability of cells in the lateral amygdala, evidenced by increased c-Fos labelling.

Finally, we investigated the impact of ELS on astrocytes in the lateral amygdala revealing changes in specific proteins associated with morphological reorganisation and astrocyte network function. ELS resulted in decreased frequency and amplitude in astrocyte calcium activity. To directly implicate astrocytes with behavioural dysfunction, we used two distinct viral approaches to mimic stress-induced astrocyte dysfunction specifically in the lateral amygdala. Impairment of astrocyte network function, or decreasing calcium activity, recapitulated ELS-induced fear generalisation, synaptic, and excitability phenotypes, supporting the hypothesis that astrocytes play an influential role in the effects of stress on neural circuits and behaviour. Together, these findings identify astrocytes as central elements regulating amygdala-dependent affective memory and highlight astrocytes as putative targets for the treatment of stress disorders.

## ELS increases blood corticosterone and induces anxiety-like behaviours

We employed an ELS paradigm which combines limited bedding and nesting materials as well as maternal separation from postnatal days 10–17 (Figure 1A) and has been shown to induce lifelong stress susceptibility (Peña et al., 2017). We first set out to determine the impact of this ELS paradigm on stress hormone levels across our experimental window. Taking trunk blood from mice across several litters at different time points in the ELS paradigm – pre-stress (P10), end of ELS paradigm (P17), at the start (P45), and end of our experimental window (P70) – we report that this ELS paradigm induces a latent increase in blood corticosterone with a significant increase occurring only in late adolescence P45, long after the termination of the stress paradigm (Figure 1B).

Next, we investigated whether this ELS paradigm results in long-term behavioural change, beginning with anxiety-like behaviours. We found that while there were no changes in behaviour in the open-field task (Figure 1D and E), we did see an increase in locomotor activity, that is, distance travelled, following ELS (Figure 1F). Using the elevated plus maze we, report increased anxiety-like behaviour with an increase in time spent in the closed arms and a reduction in time spent in the open

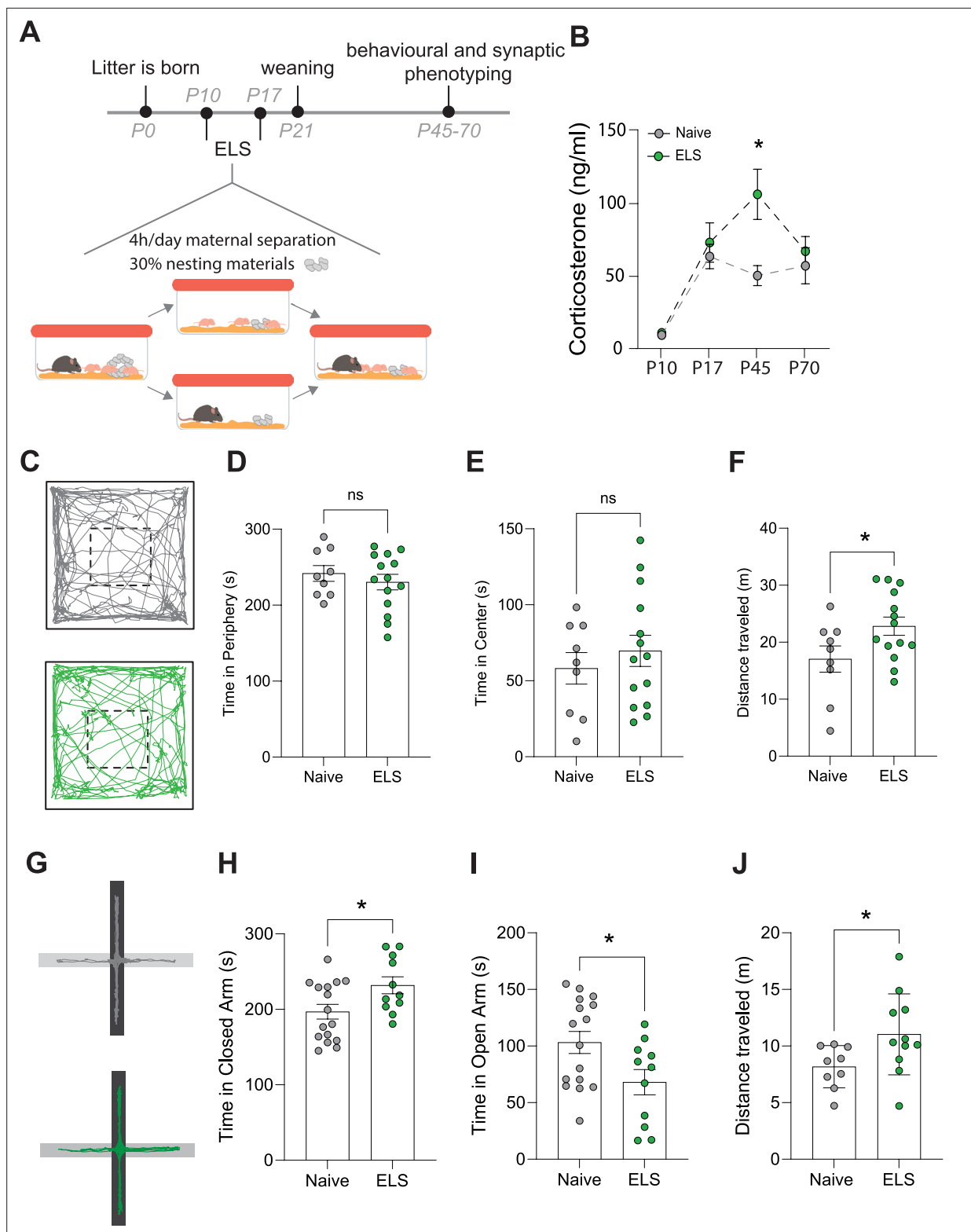


**Figure 1.** Effects of early-life stress (ELS) on anxiety-like behaviour. **(A)** Timeline of ELS and behavioural assays. **(B)** Serum corticosterone levels are increased during adolescence, following ELS.  $p=0.01$ , naive  $N = 9$ , ELS  $N = 11$  mice. **(C)** Representative movement tracks of naive (grey) and ELS (green) mice in open-field task. **(D)** No significant difference in time spent in the periphery of open-field maze following ELS.  $p=0.4591$ , naive  $N = 9$ , ELS  $N = 14$  mice. **(E)** No significant difference in time spent in the centre of open-field maze following ELS.  $p=0.4591$ , naive  $N = 9$ , ELS  $N = 14$  mice. **(F)** Total distance travelled during open-field test was increased in ELS mice.  $p=0.04$ , naive  $N = 9$ , ELS  $N = 14$  mice. **(G)** Representative locomotor tracks in

Figure 1 continued on next page

Figure 1 continued

elevated plus maze in naïve and ELS mice, black segment represents closed arms with grey arms representing open arms. (H) ELS mice had increased time spent in closed arms  $p=0.0276$ , naïve  $N = 18$ , ELS  $N = 11$  mice. (I) ELS mice had decreased time spent in open arms  $p=0.0276$ , naïve  $N = 18$ , ELS  $N = 11$  mice. (J) Total distance travelled during elevated plus maze test was increased by ELS.  $p=0.02$ , naïve  $N = 9$ , ELS  $N = 11$  mice. See **Supplementary file 1** for detailed statistical summaries.

arms of the maze (**Figure 1H and I**). This was also accompanied by an increase in distance travelled within the maze (**Figure 1J**), similar to our findings in the open field. Increased locomotion in response to stress is consistent with previous reports (**Füzesi et al., 2016; Sharma et al., 2022**).

## Amygdala-dependent memory, plasticity, and excitability are disrupted by ELS

Considering the strong association between stress disorders, anxiety, and amygdala dysfunction, we next set out to determine whether amygdala-dependent behaviour was impacted by ELS. We specifically targeted lateral amygdala-dependent learning and memory using an auditory discriminative fear conditioning paradigm. In brief, during this behavioural task mice were first exposed to a neutral auditory cue (conditioned stimulus-; CS-) followed by a distinct auditory cue (CS+) paired with footshock (unconditioned stimulus; US). Twenty-four hours later, mice were placed in a novel environment to remove contextual triggers and exposed to auditory cues from the previous day without footshock (**Figure 2B**). Memory precision was measured using per cent time freezing during presentation of neutral (CS-) and conditioned (CS+) auditory cues. We report that mice accurately learn this task and can readily distinguish between neutral and conditioned cues (**Supplementary file 1**).

Using this paradigm, we observed no effect of stress on freezing responses to the CS- presentations during conditioning (**Figure 2C**, grey area), ruling out ELS-induced hypersensitivity or hypervigilance to novel auditory cues. We also found that fear acquisition, evidenced by freezing to the CS+/US pairing, was unaffected by ELS (**Figure 2C**). In contrast, memory recall was affected with ELS mice exhibiting enhanced fear responses to neutral cues (CS-; **Figure 2D**, grey area), with no difference in freezing to conditioned cues (CS+; **Figure 2D**) compared to naïve mice. Additional analysis comparing average freezing responses to all tone presentations of CS- and CS+ supported these observations with no differences between naïve and ELS during conditioning (**Figure 2—figure supplement 2A**); while during memory recall ELS mice showed enhanced freezing to CS- presentations compared to naïve counterparts with no difference in freezing to CS+ (**Figure 2—figure supplement 2B**).

ELS-induced enhancement of fear responses to neutral cues is indicative of fear generalisation, a common stress-related behavioural phenotype conserved between rodents and humans (**Asok et al., 2018; Dymond et al., 2015**). This behavioural observation is more clearly depicted using a discrimination index (DI) that takes into account freezing responses to neutral and conditioned cues. Using this measure,  $DI > 0$  reflects accurate discrimination,  $DI = 0$  no discrimination, and  $DI < 0$  reflects a discrimination error, that is, higher freezing to the neutral than conditioned cue. Using this index, we confirm a decrease in fear discrimination in ELS mice compared to naïve mice (**Figure 2E**). Together these data reveal long-term behavioural changes with ELS enhancing affective responses resulting in fear generalisation in adult mice.

Investigation of potential sex effects revealed no differences between naïve male and female mice in this paradigm, with both sexes showing equal performance in learning (**Figure 2—figure supplement 1A**), memory (**Figure 2—figure supplement 1B**), and auditory discrimination (**Figure 2—figure supplement 1C**). In ELS mice, we report a sex-dependent effect on fear acquisition, with female mice exhibiting increased freezing responses to CS+/US pairing compared to males (**Figure 2—figure supplement 1D**). Despite this, both sexes show equal performance during memory recall and auditory discrimination (**Figure 2—figure supplement 1E and F**).

Auditory fear conditioning paradigms have been correlated with the potentiation of postsynaptic responses to cortical auditory afferents, in the lateral amygdala (**Kim and Cho, 2017**). As such, we set out to determine whether ELS impacts synaptic plasticity in cortico-amygdala circuits using acute brain slice electrophysiology and recorded field excitatory postsynaptic potentials (fEPSPs) by stimulating cortical inputs from the external capsule (**Figure 2F**). We report that ELS impaired long-term potentiation (LTP) of synaptic transmission in this cortico-amygdala circuit (**Figure 2G and H, Figure 2—figure supplement 2**). This synaptic observation is consistent with findings using distinct stress paradigms

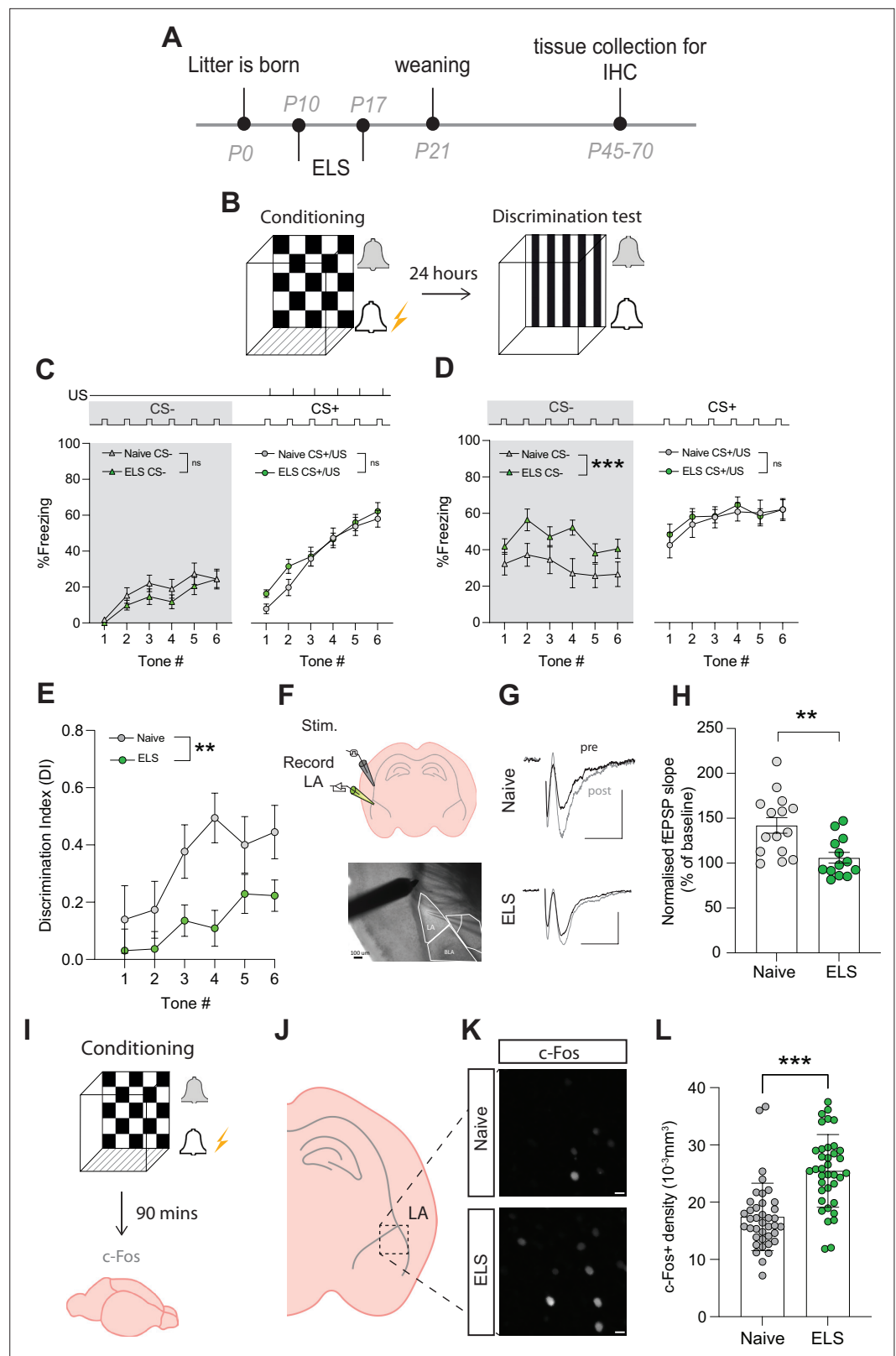


**Figure 2.** Early-life stress (ELS) alters fear memory, synaptic plasticity, and neural excitability. **(A)** Experimental timeline. **(B)** Timeline of auditory discriminative fear conditioning paradigm. **(C)** ELS did not affect % freezing to neutral and aversive auditory cues during learning. Naive N = 20, ELS N = 17. **(D)** % time freezing during presentation of neutral auditory cue (CS-; p=0.0002) and aversive cue (CS+; p=0.99). Naive N = 20, ELS N = 17. *Figure 2 continued on next page*

Figure 2 continued

(E) Discrimination Index was impaired by ELS.  $p=0.004$ , naïve  $N = 20$ , ELS  $N = 17$ . (F) Schematic representation of electrode placement in slice electrophysiology experiment (top) with DIC image below. (G) Representative EPSP traces from naïve (top) and ELS (bottom) brain slices during baseline (black trace) and after LTP stimulation (grey trace). Scale bars = 0.5 mV and 10 ms. (H) LTP was impaired by ELS.  $p=0.002$ , naïve  $N = 15$ , ELS  $N = 13$ . (I) Diagram of procedure for c-Fos staining experiments. (J) Brain slices containing lateral amygdala (LA) were selected for c-Fos staining. (L) Region of interest extracted from full amygdala image. Scale bars = 10  $\mu\text{m}$ . (K) c-Fos-positive cell density was increased by ELS.  $p<0.0001$ , naïve  $n = 39$  slices  $N = 10$  mice, ELS  $n = 37$  slices  $N = 10$  mice. See **Supplementary file 1** for detailed statistical summaries.

The online version of this article includes the following figure supplement(s) for figure 2:

**Figure supplement 1.** Effect of sex on amygdala-dependent learning and memory in naïve and ELS mice.

**Figure supplement 2.** Sex-dependent effects of early-life-stress (ELS) on neuronal excitability following fear conditioning.

**Figure supplement 3.** Astrocytic expression of c-Fos after fear conditioning.

---

(Murphy-Royal et al., 2020) and highlights the important influence of stress on synaptic function across various brain regions.

Fear learning and memory in the lateral amygdala have also been correlated with the allocation of a small number of neurons to a fear engram (Josselyn et al., 2015). These engrams are thought to be a possible neural substrate for memory, and their formation depends on neural excitability levels at the moment of acquisition (Rashid et al., 2016; Ramsaran et al., 2023). As both glucocorticoid injections or acute stress have been shown to increase engram size and enhance fear generalisation (Lesuis et al., 2021; Lesuis et al., 2025), we set out to determine whether ELS results in memory changes due to alterations in putative engram recruitment. We collected brain tissue 90 min after conditioning (Figure 2I) and carried out immunostaining for the immediate early gene c-Fos, a commonly used activity marker, in the lateral amygdala (Figure 2J–L, Figure 2—figure supplement 2D and E). Fear acquisition in ELS mice resulted in a significant increase in c-Fos density, suggestive of increased excitability levels. These results are consistent with reports of c-Fos density inversely correlating with memory accuracy (Ramsaran et al., 2023). Further investigation of potential sex differences revealed that while there were no differences in c-Fos densities between naïve female and male animals (Figure 2—figure supplement 2F), we observed a significantly higher c-Fos density in ELS male mice compared to females following fear acquisition (Figure 2—figure supplement 2G).

Recently, astrocytes have been reported to be recruited to fear engrams during a hippocampus-dependent learning and memory task (Williamson et al., 2024). As such, we quantified the percentage of astrocytes expressing the activity marker c-Fos following fear conditioning in mice and report similar values to those found in the hippocampus (Figure 2—figure supplement 3A and B) suggestive of modest recruitment of astrocytes in amygdala-dependent memory engrams.

## ELS induces persistent changes in astrocytes

To determine the influence of ELS on astrocytes in the lateral amygdala, we carried out immunostaining on brain slices taken from a separate cohort of naïve and ELS mice. We first investigated whether increased blood corticosterone affects glucocorticoid receptor (GR) expression and localisation in astrocytes. Using immunostaining, we confirmed that this hormone receptor is abundantly expressed in lateral amygdala astrocytes (Figure 3B). We further investigated the subcellular localisation of GR within astrocytes. When inactivated GRs are restricted to the cytosol, upon binding to agonists such as corticosterone, however, GRs can translocate to the nucleus to influence gene expression (de Kloet et al., 2005). Calculating a ratio of cytosolic vs nuclear GR in astrocytes as a proxy for activity, we found an increase in the nuclear fraction of GR in astrocytes following ELS (Figure 3C), suggestive of increased activation of glucocorticoid signalling in lateral amygdala astrocytes following ELS.

To assess putative changes in astrocyte structure, we investigated expression of the intermediate filament protein glial fibrillary acidic protein (GFAP; Figure 3D and E) and found a significant decrease in normalised GFAP fluorescence intensity in the lateral amygdala following ELS (Figure 3F). While functional consequences of GFAP changes are difficult to define, we interpret these modifications in GFAP expression to be indicative of an astrocytic response to stress. We next targeted astrocyte-specific proteins with known roles in influencing synaptic function including Cx43, a gap junction

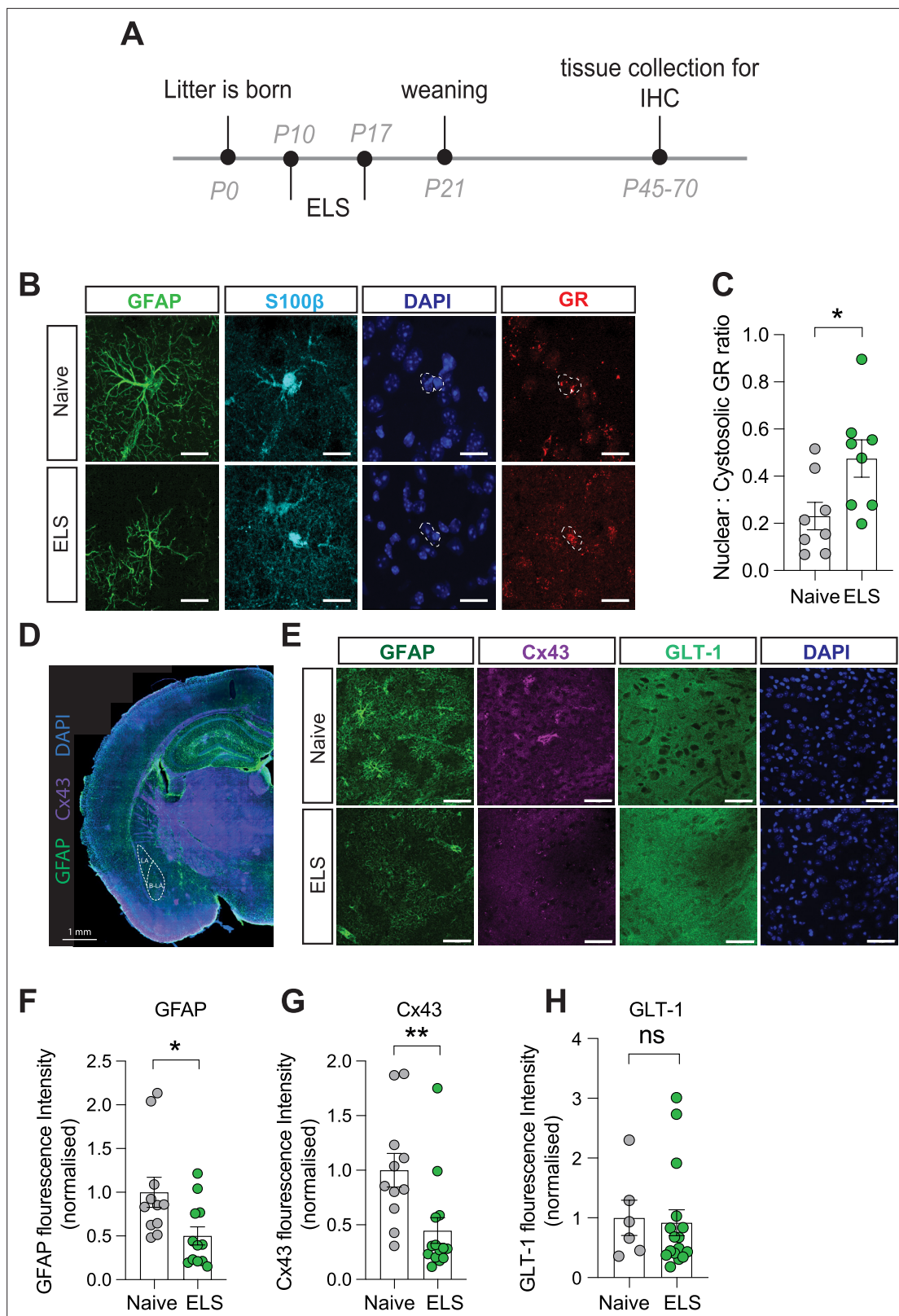


**Figure 3.** Long-term astrocyte dysfunction after early-life stress. **(A)** Experimental timeline. **(B)** Representative immunostaining of GFAP, S100 $\beta$ , GR, DAPI, and GR/DAPI merge in naïve and early-life stress (ELS) conditions. Scale bars = 20  $\mu$ m. **(C)** Nuclear/cystolic GR ratio in astrocytes was increased after ELS.  $p=0.026$ , naïve  $N=8$ , ELS  $N=8$ . **(D)** Representative slide scan image of immunostaining for astrocyte proteins GFAP and Cx43. **(E)** Representative immunostaining of GFAP, Cx43, GLT-1, and DAPI in naïve and ELS conditions. Scale bars = 50  $\mu$ m **(F)** GFAP staining was reduced in

Figure 3 continued on next page

Figure 3 continued

ELS mice.  $p=0.02$ , Naïve  $N = 11$ , ELS  $N = 12$ . (G) Cx43 staining was decreased in ELS mice.  $p=0.008$ , naïve  $N = 11$ , ELS = 14. (H) GLT-1 expression was unchanged by ELS.  $p=0.8$ , naïve  $N = 6$ , ELS  $N = 16$ . See **Supplementary file 1** for detailed statistical summaries.

The online version of this article includes the following figure supplement(s) for figure 3:

**Figure supplement 1.** Absence of sex-differences in GFAP and Cx43 in naïve and ELS mice.

protein that composes astrocyte networks (Giaume *et al.*, 2010) and the glutamate transporter GLT-1, responsible for the efficient clearance of glutamate from the synaptic cleft (Kruyer *et al.*, 2022; Figure 3D and E).

We observed a decrease in fluorescence intensity for the gap junction protein Cx43 (Figure 3G) while expression of the glutamate transporter GLT-1 remained unaffected by ELS (Figure 3H). We did not observe any significant sex differences in the expression of GFAP or Cx43 in control or ELS conditions, with similar expression levels in naïve and the same effect of stress on these proteins in both male and female mice (Figure 3—figure supplement 1A and B). These data suggest that astrocytes mount a specific response to ELS which could result in discrete changes in astrocyte network function such as the uncoupling of the astrocytic Cx43 gap junction networks in the lateral amygdala.

### ELS impairs astrocyte calcium activity

While the ELS-induced changes in astrocyte protein expression are indicative of functional modifications, this cannot be assumed and needs to be tested. We chose to assess potential stress-induced changes in astrocyte calcium activity employing the membrane-tethered calcium sensor Ick-GCaMP6f. Lateral amygdala astrocytes were specifically targeted using local injection of viral constructs with GCaMP6f expression driven by the GfaABC1D promoter. Two-photon laser scanning microscopy was used in acute brain slices a minimum of 2 weeks following virus injection (Figure 4A), allowing for quantification of dynamic elevations in intracellular calcium in astrocytic processes in naïve (Figure 4B and C) and ELS mice (Figure 4D and E). Data was analysed using the AQUA2 pipeline, allowing for accurate and unbiased analysis of spatial and temporal dynamics of astrocyte calcium activity (Mi *et al.*, 2024).

We report that ELS results in astrocyte calcium hypofunction, evidenced by decreased calcium event frequency (Figure 4F and G), amplitude (Figure 4H and I), and size of individual events (Figure 4J and K). Additionally, we observed a modest increase in rise time of calcium transients (Figure 4L and M) with no significant change in event duration (Figure 4N and O) or decay time (Figure 4P and Q). Together, these results are suggestive of astrocyte hypofunction following ELS.

Unexpectedly, our experiments revealed sexual dimorphism in astrocytic calcium dynamics in the lateral amygdala between naïve female and male mice. Specifically, we found that naïve female mice exhibited larger event amplitudes (Figure 4—figure supplement 1A and B), event area (Figure 4—figure supplement 1D and E), and rise time (Figure 4—figure supplement 1G and H) compared to naïve male mice. Interestingly, all sex differences were suppressed by stress with ELS-induced decrease in astrocyte activity normalising all parameters between sexes (Figure 4—figure supplement 1A, C, D, E, G, and I).

No sex differences were observed for event frequency (Figure 4—figure supplement 1J–L), duration (Figure 4—figure supplement 1M–O), or decay time (Figure 4—figure supplement 1P–R) in any conditions.

### Astrocyte dysfunction alone phenocopies the effects of ELS on fear generalisation, synaptic plasticity, and excitability

To implicate astrocytes in the cellular and behavioural effects of ELS, we carried out a series of genetic loss-of-function experiments, specifically targeting astrocytes in the lateral amygdala using viral approaches (Figure 5A–C, Figure 5—figure supplement 1A). Based on the putative astrocyte network dysfunction we identified in fixed tissue (Figure 3G), we targeted astrocyte network function by overexpressing a dominant negative Cx43 (dnCx43). We have previously shown this manipulation to completely occlude functional coupling between neighbouring astrocytes by introducing a point mutation that blocks the pore of gap junction channels (dnCx43) (Murphy-Royal *et al.*, 2020). Second, to mimic the impact of ELS on astrocyte calcium activity (Figure 4), we used a calcium extruder



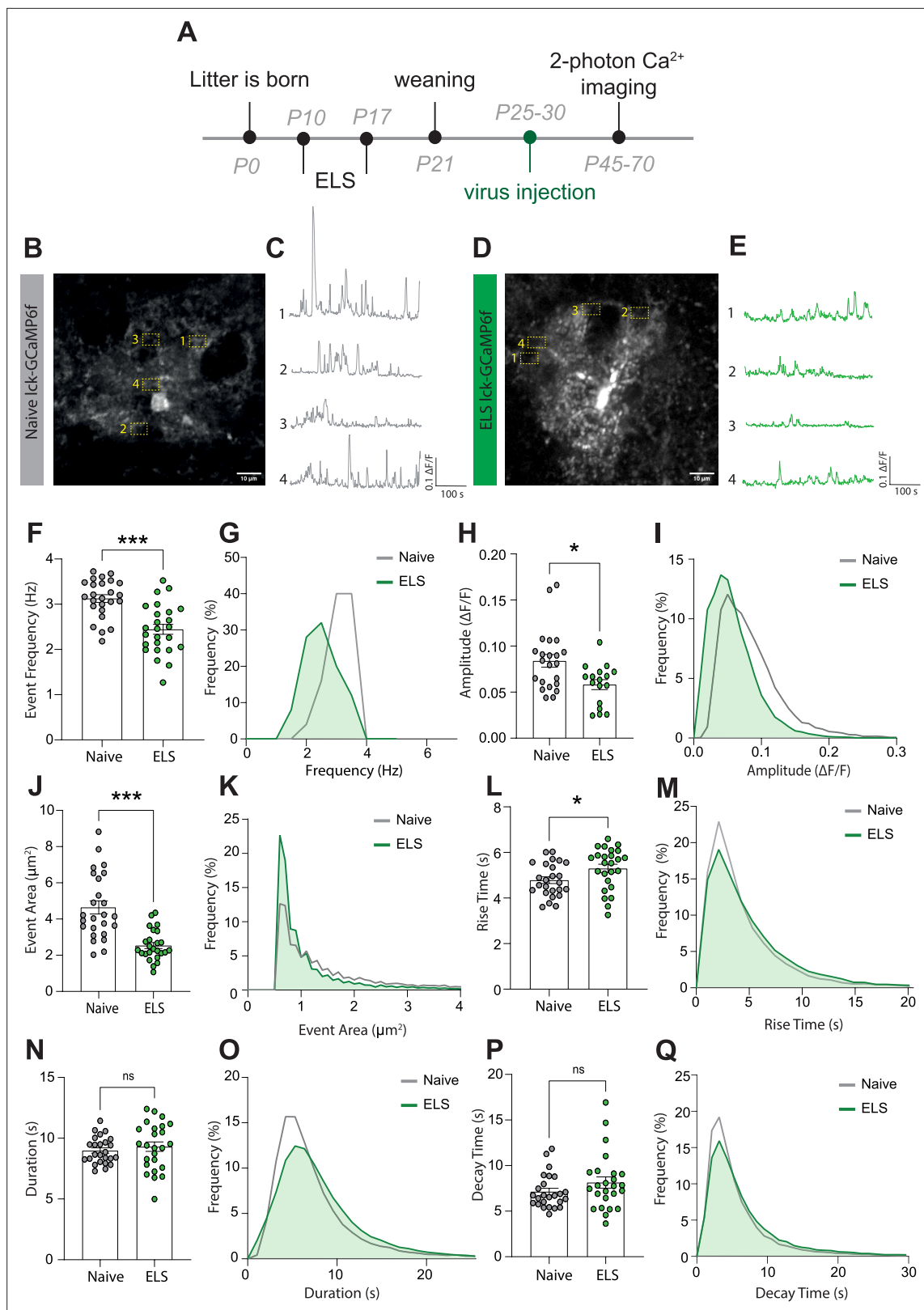


**Figure 4.** Early-life stress (ELS) induces a hypofunction in lateral amygdala astrocyte calcium signalling. **(A)** Experimental timeline including age of viral injection and experimental window for two-photon calcium imaging. **(B)** Representative image of a Ick-GCaMP6f-expressing astrocyte in the lateral amygdala with four regions of interest from a naïve animal. Scale bar = 10  $\mu\text{m}$ . **(C)** Representative calcium-signalling traces from four regions of interest shown in **(B)**. **(D)** Representative image of a Ick-GCaMP6f-expressing astrocyte in the lateral amygdala with four regions of interest from an ELS animal.

Figure 4 continued on next page

Figure 4 continued

Scale bar = 10  $\mu$ m. (E) Representative calcium-signalling traces from four regions of interest shown in (D). (F) Frequency of calcium events was decreased lateral amygdala astrocytes after ELS,  $p < 0.0001$ , naïve  $n = 25$  astrocytes from  $N = 8$  animals, ELS  $n = 25$  astrocytes from  $N = 7$  animals. (G) Frequency distribution of calcium event frequency from naïve (grey line) and ELS (green line) animals. (H) Amplitude of calcium events was decreased after ELS,  $p = 0.0165$ , naïve  $n = 22$  astrocytes from  $N = 8$  animals, ELS  $n = 17$  astrocytes from  $N = 7$  animals. (I) Frequency distribution of calcium event amplitude from naïve (grey line) and ELS (green line) animals. (J) Area of calcium events was decreased after ELS,  $p < 0.0001$ , naïve  $n = 25$  astrocytes from  $N = 8$  animals, ELS  $n = 25$  astrocytes from  $N = 7$  animals. (K) Frequency distribution of event area from naïve (grey line) and ELS (green line) animals. (L) Rise time of calcium events was increased following ELS,  $p = 0.0311$ , naïve  $n = 25$  astrocytes from  $N = 8$  animals, ELS  $n = 25$  astrocytes from  $N = 7$  animals. (M) Frequency distribution of calcium event rise from naïve (grey line) and ELS (green line) animals. (N) Calcium event duration was unchanged by ELS,  $p = 0.4740$ , naïve  $n = 25$  astrocytes from  $N = 8$  animals, ELS  $n = 25$  astrocytes from  $N = 7$  animals. (O) Frequency distribution of calcium event duration from naïve (grey line) and ELS (green line) animals. (P) Decay time of calcium events was unaltered by ELS,  $p = 0.2164$ , naïve  $n = 25$  astrocytes from  $N = 8$  animals, ELS  $n = 25$  astrocytes from  $N = 7$  animals. (Q) Frequency distribution of calcium event decay time duration from naïve (grey line) and ELS (green line) animals.

The online version of this article includes the following figure supplement(s) for figure 4:

**Figure supplement 1.** Early-life-stress suppresses sexual dimorphism in lateral amygdala astrocyte calcium activity.

pump (hPMCA2/b, a.k.a. CalEx) (Institoris et al., 2022; Yu et al., 2018) that we validated to show that expression of this pump in lateral amygdala astrocytes (Figure 5—figure supplement 2A–E) effectively reduces frequency (Figure 5—figure supplement 2F) and amplitude (Figure 5—figure supplement 2G) of astrocyte calcium events without affecting event size, duration, rise time, or decay (Figure 5—figure supplement 2H–K). This manipulation closely mimics the effects of ELS on astrocyte calcium activity, allowing us to parse the precise contribution of astrocyte activity in behaviour.

Initially, we screened for changes in anxiety-like behaviours using the elevated plus maze and report no impact of lateral amygdala-specific astrocyte manipulation on the time spent in the open versus closed arms or in total distance travelled (Figure 5—figure supplement 3A–C) nor in time spent in the periphery versus the middle of the open-field maze or in total distance travelled (Figure 5—figure supplement 3D–F). Next, using auditory discriminative fear conditioning paradigm, we found that learning was unaffected by astrocyte dysfunction (Figure 5D, Figure 5—figure supplement 4A). We also report that similar to ELS, lateral amygdala astrocytic dysfunction does not lead to hypervigilance to neutral auditory cues (Figure 5D, grey area). During memory recall, however, we found that both astrocyte hypofunction manipulations enhanced fear responses to neutral cues, without affecting freezing to conditioned cues (Figure 5E, Figure 5—figure supplement 4B). This behavioural phenotype induced by astrocyte dysfunction alone, with either dnCx43 or CalEx, mimicked the effects of ELS on auditory fear discrimination, that is, enhanced fear generalisation. Accordingly, quantification of DI revealed an impairment in discriminative fear memory in both dnCx43 and CalEx conditions, compared to viral control (Figure 5F). This effect was dependent on the increase in freezing to the neutral cue with freezing responses to the aversive tone being unaltered by astrocytic dysfunction (Figure 5—figure supplement 4B). Taken together, these data directly implicate astrocytes in valence processing in the lateral amygdala and suggest a potential link between ELS and astrocyte dysfunction.

Investigation of potential sex differences in these genetic manipulations of astrocyte function revealed that the impact of CalEx on discrimination memory was more robust in female mice compared to males (Figure 5—figure supplement 4C). In the case of dnCx43, no differences were observed between females and males (Figure 5—figure supplement 4D).

Next, we set out to determine whether astrocyte dysfunction also mirrored the cellular and synaptic changes observed in ELS. Using acute brain slice electrophysiology, we report an occlusion of LTP in both CalEx and dnCx43 conditions (Figure 5G). In line with fear memory and synaptic plasticity changes, we also report that astrocyte dysfunction directly influences neural excitability with increased c-Fos density following fear conditioning in both CalEx and dnCx43 compared to control virus (Figure 5H and L). No sex differences were observed for c-Fos densities in eGFP- (Figure 5—figure supplement 5A and D) or CalEx-expressing mice (Figure 5—figure supplement 5B and E). dnCx43 expression, however, resulted in higher c-Fos density in female mice compared to male counterparts (Figure 5—figure supplement 5F).

Globally, these data highlight astrocytes as critical regulators of lateral amygdala function and output with astrocyte integrity essential for regulating synaptic plasticity, neural excitability, and of brain region-dependent behaviour (Figure 6).

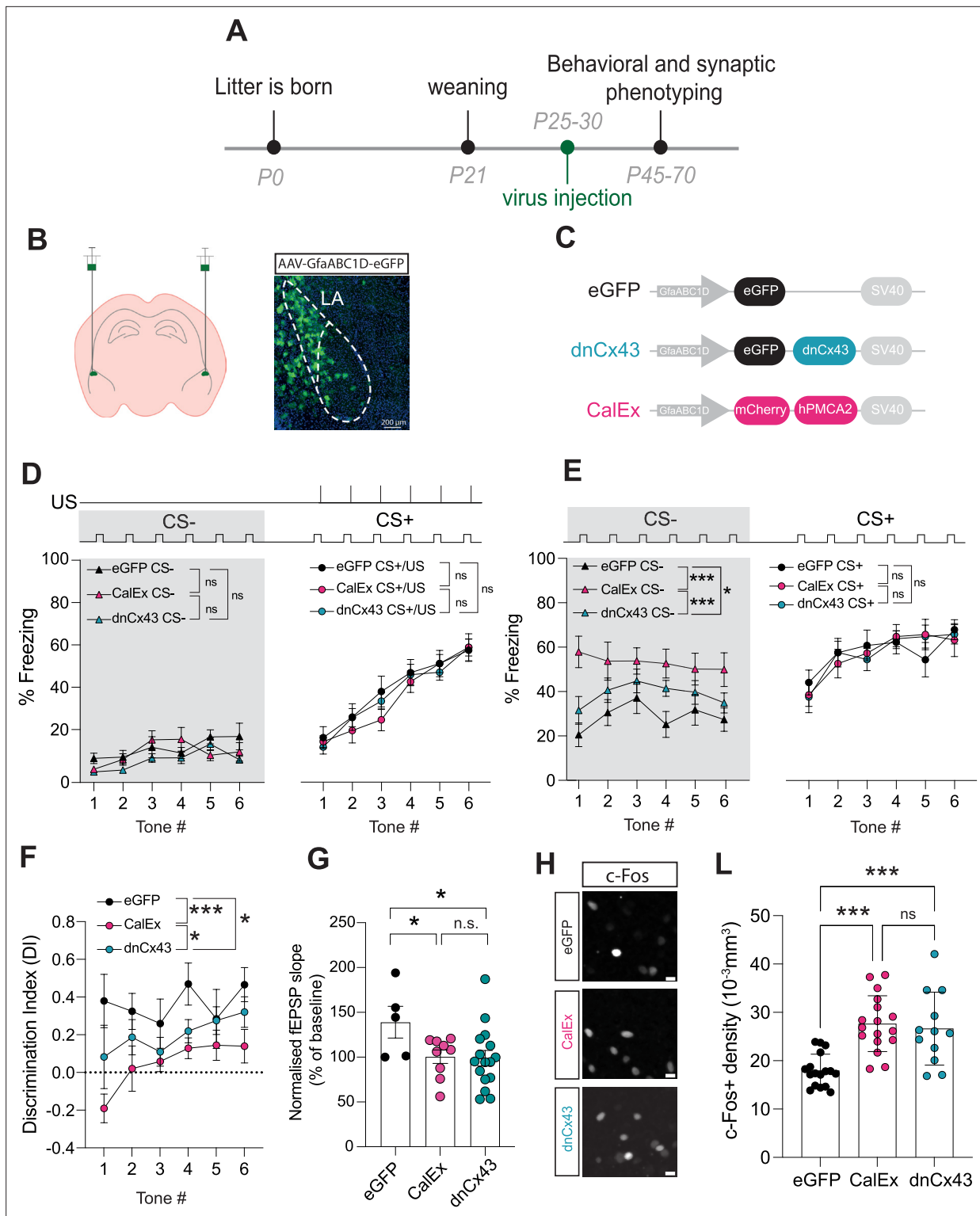


**Figure 5.** Astrocyte dysfunction mimics the effects of early-life stress (ELS) on behaviour, synapses, and neural excitability. **(A)** Experimental timeline. **(B)** Representative image showing localisation of viral vector in lateral amygdala. **(C)** Viral constructs used to manipulate astrocyte function. **(D)** Astrocyte dysfunction did not affect % freezing to neutral and aversive auditory cues during learning. eGFP N = 12, CalEx N = 11, dnCx43 N = 17 mice. **(E)** % time freezing during presentation of neutral auditory cue (CS-) was increased with astrocyte dysfunction (eGFP vs CalEx:  $p < 0.0001$ ; eGFP vs dnCx43:  $p = 0.029$ ; CalEx vs dnCx43:  $p = 0.0005$ ) with no impact on % freezing to aversive cue (CS+). eGFP N = 12, CalEx N = 11, dnCx43 N = 17 mice. **(F)** Discrimination Indexes were impaired by astrocyte dysfunction. eGFP vs CalEx:  $p < 0.0001$ ; eGFP vs dnCx43:  $p = 0.013$ ; CalEx vs dnCx43:  $p = 0.03$ . eGFP N = 12, CalEx N = 11, dnCx43 N = 17 mice.

Figure 5 continued on next page

Figure 5 continued

= 11, dnCx43 N = 17 mice. (G) Astrocyte dysfunction occluded the induction of LTP. eGFP vs CalEx:  $p=0.04$ ; eGFP vs dnCx43:  $p=0.02$ ; CalEx vs dnCx43:  $p=0.88$ . eGFP N = 5, CalEx N = 9, dnCx43 N = 16. (H) Representative c-Fos staining in the lateral amygdala in control (eGFP), CalEx, and dnCx43 conditions. Scale bars = 10  $\mu\text{m}$ . (L) c-Fos-positive cell density was increased with astrocyte dysfunction. eGFP vs CalEx:  $p<0.0001$ ; eGFP vs dnCx43:  $p=0.0005$ ; CalEx vs dnCx43:  $p=0.88$ . eGFP n = 17 slices N = 5 mice, CalEx n = 17 slices N = 5 mice, dnCx43 n = 12 slices N = 5 mice.

The online version of this article includes the following figure supplement(s) for figure 5:

**Figure supplement 1.** Viral targeting of lateral amygdala astrocytes.

**Figure supplement 2.** CalEx expression in lateral amygdala astrocytes suppresses calcium activity and closely mimics the effects of ELS on calcium activity.

**Figure supplement 3.** Impact of genetic manipulation of lateral amygdala astrocyte function on anxiety-related behaviours.

**Figure supplement 4.** Expression of CalEx, but not dnCx43, in lateral amygdala astrocytes results in sexually dimorphic effects on discrimination.

**Figure supplement 5.** Expression of dnCx43, but not CalEx, in lateral amygdala astrocytes influences neuronal excitability in sex-specific manner following fear conditioning.

## Discussion

In this study, we investigated the potential roles of astrocytes in cellular and behavioural dysfunctions associated with ELS. Using a rodent model of ELS that employs maternal separation and limited bedding, we report increased blood glucocorticoid levels associated with heightened anxiety-like behaviours. These endocrine and behavioural changes were accompanied by impaired discriminative

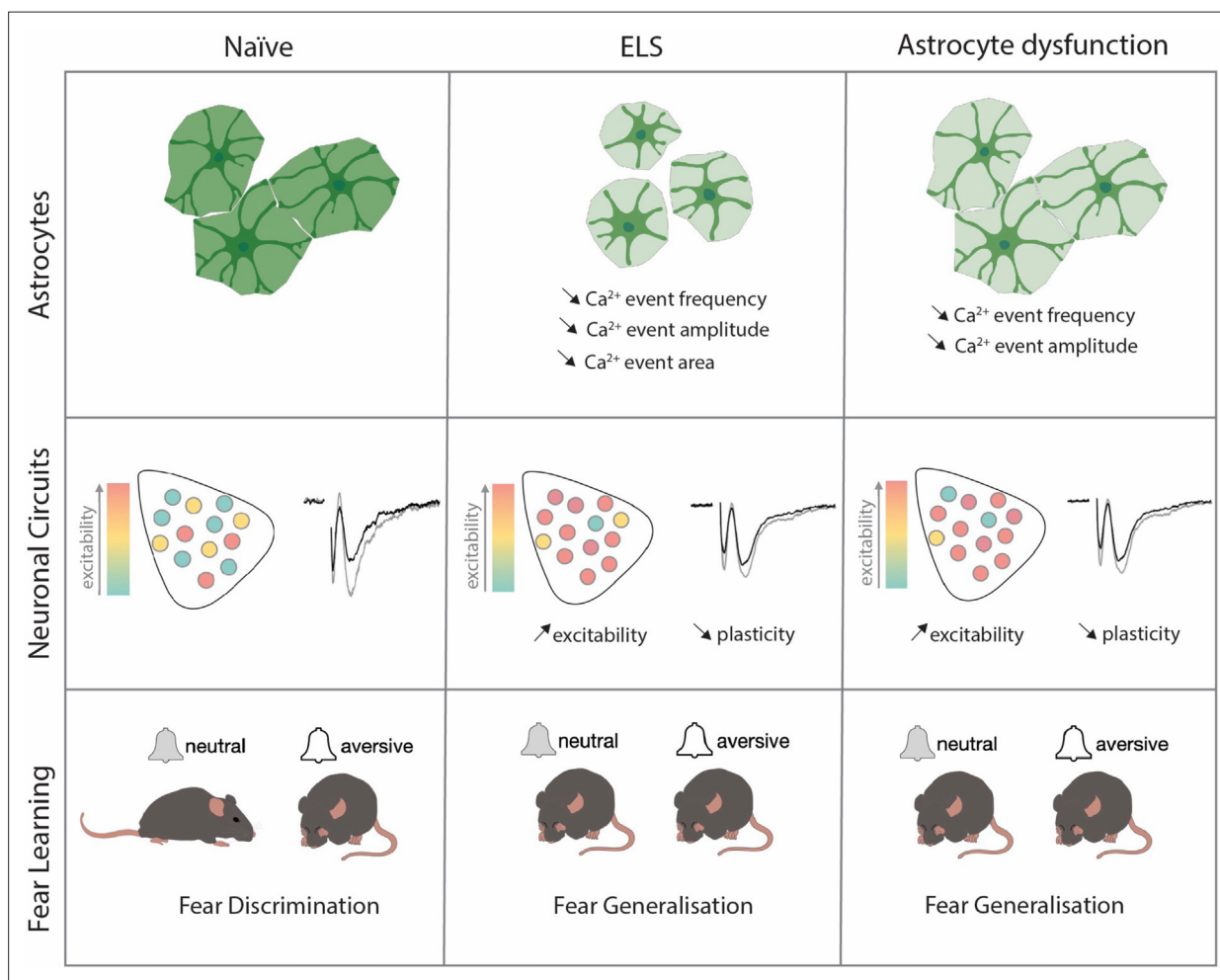


**Figure 6.** The effects of early-life-stress on astrocytic function, neuronal excitability, and fear memory are fully recapitulated by viral manipulations of lateral amygdala astrocytes.

fear memory in an amygdala-dependent auditory discrimination task. More precisely, we observed that ELS mice displayed increased fear responses to neutral cues with no change in freezing responses to conditioned stimuli. These behavioural changes were further associated with alterations on the cellular scale including synaptic plasticity and neuronal excitability. Investigating contributions of non-neuronal cells, we found robust changes in lateral amygdala astrocytes following ELS comprising increased GR translocation to the nucleus and decreased expression of key astrocyte network proteins. Functionally, we observed astrocyte hypoactivity with decreased frequency, amplitude, and size of calcium events following ELS.

To link astrocyte dysfunction with cellular, synaptic, and behavioural changes, we genetically targeted lateral amygdala astrocytes to mimic the effects we found in ELS. Astrocyte dysfunction alone, either decreasing gap junction coupling or reducing astrocyte calcium activity, phenocopied the effects of ELS across excitability, synaptic, and behavioural scales. Astrocytes have long been shown to be critical for memory formation, with the vast majority of studies reporting that astrocyte dysfunction impairs memory across various brain regions (*Robin et al., 2018; Yu et al., 2018; Depaauw-Holt et al., 2024; Sun et al., 2012*). Here, we show that astrocyte dysfunction in the lateral amygdala effectively impairs discriminative fear memory evidenced by fear generalisation, that is, the inappropriate expression of fear towards stimuli of neutral valence. These data reveal that astrocytes are critical for the appropriate behavioural responses to emotionally salient cues and provide evidence supporting the recently proposed contextual guidance theory of astrocyte function in the brain (*Murphy-Royal et al., 2023*).

Using an ELS paradigm that coincides with peak astrocyte postnatal development (*Rurak et al., 2022; Farhy Tselnicker and Allen, 2018*), we found a latent increase in circulating glucocorticoids after ELS with peak levels appearing during late adolescence and subsiding towards adulthood. While the lack of endocrine response to stress during the stress paradigm might appear paradoxical, this ELS paradigm overlaps with the stress hyporesponsive period, a time window during which stressors fail to elicit increases in blood corticosterone levels (*Schmidt et al., 2003; Sapolsky and Meaney, 1986; Schmidt, 2019; Vázquez, 1998*). Indeed, similar to our findings, others have reported latent increases in blood corticosterone levels following ELS that were associated with increased anxiety-like behaviour (*Sharma et al., 2022*) and fear generalisation (*Elliott and Richardson, 2019*) later in life. Increased levels of blood glucocorticoids had a direct impact on astrocytes with increased translocation of GR from the cytosol to the nucleus of astrocytes following ELS, indicative of a higher levels of glucocorticoid signalling (*de Kloet et al., 2005*). While the effects of ELS on blood glucocorticoids were transient, this could have long-term consequences on protein expression levels, resulting in changes in stress susceptibility and behavioural deficits. The primary behavioural phenotype revealed by this work, that is, fear generalisation, is a common trait observed in anxiety disorders (*Dymond et al., 2015; Lissek and van Meurs, 2015; Lis et al., 2020*). As such, these findings provide further insight into the neurobiological mechanisms of stress on endocrine, cellular, and behavioural scales.

Our work builds upon a growing literature that is interested in the potential roles of astrocytes in ELS (*Vivi and Di Benedetto, 2024; Abbink et al., 2019; Gunn et al., 2013*). Here, we identified specific astrocytic impairments induced by ELS and followed up with precise genetic manipulation of these astrocyte functions in the lateral amygdala. These astrocyte-specific manipulations replicate cellular and fear generalisation phenotype observed following ELS. We did not, however, observe an anxiety-like phenotype using elevated plus maze and open field with local astrocyte manipulation which could be interpreted as a lack of amygdala astrocyte involvement in these discrete behaviours.

We found that both ELS and astrocyte dysfunction enhance neuronal excitability, assessed by local c-Fos staining in the lateral amygdala following auditory discriminative fear conditioning. One interpretation of these data is that astrocytes might tune engram formation, with astrocyte dysfunction, genetically or after stress, increasing c-Fos expression and a loss of specificity of the memory trace. In support of this notion, evidence of a cellular mechanism whereby c-Fos levels inversely correlate with memory accuracy has been recently shown in hippocampal circuits (*Asok et al., 2018*). In addition, early-life experience strongly shapes episodic memory development, with stress delaying maturation of memory processes (*Ramsaran et al., 2024*). Early-life stress has even been shown to activate specific neuronal ensembles that contribute to stress hypersensitivity (*Balouek et al., 2023*). Further support comes from recent demonstration of astrocyte-engram neuron interactions with astrocytes potentially forming part of engram stabilisation or even direct recruitment of astrocytes into engrams

(Williamson *et al.*, 2024; Kim *et al.*, 2023). Our data are in line with previous reports that have demonstrated clear roles for astrocytes in memory formation and consolidation (Martin-Fernandez *et al.*, 2017; Adamsky *et al.*, 2018; Kol *et al.*, 2020) and reveal that astrocytes participate in the neurobiological mechanisms by which stress influences emotional memory.

Our work revealed unexpected sex differences in calcium signalling in lateral amygdala astrocytes. We found astrocyte calcium events were larger in amplitude and size in female mice compared to males. This higher basal activity could explain why CalEx induced a more profound impairment in fear discrimination in female mice. Interestingly, these sex differences are eliminated by stress inducing a homogenous calcium signature between both sexes. Sex differences in astrocytic development and function is starting to gain increased attention (Depaauw-Holt *et al.*, 2024; Rurak *et al.*, 2022; González-Vila *et al.*, 2023), with much more to be learned regarding the potentially divergent functions of astrocytes in the female and male brain.

In sum, our data shed new light on the role of astrocytes as central regulators of amygdala-dependent behaviour, synaptic function, and excitability. In addition, our work suggests a key role of astrocytes in mediating stress-induced behavioural and cellular impairments, supporting the notion that astrocytic disruption is not simply downstream of neuronal dysfunction. These ideas are forcing a change in perception of how brain disorders develop, moving away from a neuro-centric cascade and placing astrocytes in the spotlight (Murphy-Royal *et al.*, 2023; Vivi and Di Benedetto, 2024; Seifert *et al.*, 2006; Lee *et al.*, 2022; Endo *et al.*, 2022; Khakh and Goldman, 2023). Collectively, these data support the hypothesis that astrocytes are key to execute the appropriate behavioural response to emotionally salient cues and underscore the potential of astrocytes as therapeutic targets in stress-related psychiatric conditions.

## Materials and methods

### Animals

All experiments were performed in accordance with the guidelines for maintenance and care of animals of the Canadian Council on Animal Care and approved by the Institutional Committee for the Protection of Animals at the Centre Hospitalier de l'Université de Montréal, protocol number CM20031CMRs. Both male and female C57BL/6J mice (Jax #000664) were used in the study, housed on a 12 hr:12 hr light:dark cycle (lights on at 06:30) with ad libitum access to food and water.

### ELS protocol

ELS was performed as previously described (Peña *et al.*, 2017). C57BL/6J pups were separated from their mothers for 4 hr per day (ZT2-ZT6) for 7 days between ages P10 and P17. During separation, pups and mothers were placed into new cages with 60% less bedding. Bedding was weighed on P10 and divided 33% into each cage (home cage, pup separation cage, and mother separation cage). Separated pups and mothers had ad libitum access to food and water and pup cages were placed on a water heating pad maintained at 34°C. After the final day of separation (P17), bedding was returned to the original amount and pups were housed with their mothers until weaning at P21.

### Behavioural assays

#### Auditory discriminative fear conditioning

Mice between ages P45-70 were used. Four days prior to behavioural testing, mice were single housed in individual cages. Two days later, mice were handled for approximately 10 min by hand and mobilisation tube. On the first day of ADFC, single housed mice were left for 1 hr in behavioural room to habituate prior to the start of the conditioning assay.

#### Conditioning

Mice were first exposed to a neutral stimulus (CS-; white noise, 20 s) repeated six times. After a 2-min interval, mice were exposed to a tone which becomes the conditioned stimulus (CS+; 12 kHz tone, 20 s) as it co-terminates with a mild foot shock (US; 0.5 mA, 2 s) delivered in the last 2 s of tone presentation (repeated six times). Conditioning was carried out in chamber with checkered walls that was cleaned with 70% ethanol between animals.

## Memory recall

Then, 24 hr after conditioning, mice were exposed to CS- and CS+ (counterbalanced) in a novel environment characterised by stripped walls and a white floor covering, cleaned with 0.5% hydroperoxide between animals. Fear learning was quantified by the percentage of time spent freezing to CS- and CS+/US during the conditioning phase. Fear memory was quantified by the percentage time freezing to CS- or CS+ following presentation in the memory-recall phase. A DI was calculated comparing fear responses to CS+ and CS- using the following formula:

$$\text{Discrimination Index (DI)} = \frac{(\text{CS}^+ \text{ Freezing}) - (\text{CS}^- \text{ Freezing})}{(\text{CS}^+ \text{ Freezing}) + (\text{CS}^- \text{ Freezing})}$$

## Open-field task

This task comprised of a total of 5 min and during that time the mice were left to freely explore the OFT apparatus, a white plexiglass box measuring 38 × 38 cm. During the task, mice were filmed, and the time spent in distinct parts of the box, that is, centre and periphery were quantified using AnyMaze software (Stoelting). The total time spent in the centre was used as a quantification of anxiety-like behaviour, where more time in the centre represented less anxiety-like behaviour and the total distance travelled was measured to quantify locomotor changes.

## Elevated plus maze

This task comprised of a total of 5 min during which mice were removed from their cages and placed at the centre of the four arms of the maze, facing an open arm. Mice were video recorded, and these videos were analysed using AnyMaze software (Stoelting) which quantified the time spent (s) in closed arms or open arms during the 5 min testing period. Anxiety-like behaviour was quantified by ratio of time spent in open vs closed arms.

## Acute brain slice preparation

Coronal slices containing lateral amygdala were obtained from mice between P45 and 70. Animals were anaesthetised with isoflurane and the brain was rapidly excised and placed in ice-cold choline-based cutting solution saturated with 95% O<sub>2</sub> and 5% CO<sub>2</sub> containing the following (in mM): 120 choline chloride, 3 KCl, 1.25 NaH<sub>2</sub>PO<sub>4</sub>, 26 NaHCO<sub>3</sub>, 8 MgCl<sub>2</sub>, 20 glucose, pH 7.2, and 295 mOsmol. Slices (300 µm thick) were cut on a vibratome (Leica VT1200, Nussloch, Germany). Slices were transferred to oxygenated artificial CSF (ACSF) at 32 ± 0.5°C for 30 min containing the following (in mM): 130 NaCl, 2.5 KCl, 1.25 NaH<sub>2</sub>PO<sub>4</sub>, 26 NaHCO<sub>3</sub>, 10 glucose, 1.3 MgCl<sub>2</sub>, 2 CaCl<sub>2</sub>, pH 7.3–7.4, and 300–305 mOsmol, then allowed to recover for at least 30 min before recordings in oxygenated ACSF at room temperature (RT). For experiments, the slices were transferred to a recording chamber where they were perfused (2 ml/min) with ACSF at 32°C for the course of the experiment. Slices were used for a maximum of 6 hr after cutting.

## Electrophysiology

Extracellular fEPSPs were recorded in current-clamp mode with a pipette filled with ACSF placed in the lateral part of the amygdala. Monosynaptic EPSPs were elicited by stimulation of cortical afferences with a tungsten concentric bipolar electrode (World Precision Instruments). LTP was induced using a theta burst stimulation protocol consisting of four pulses at 100 Hz repeated at 5 Hz intervals for 10 s. Signals were amplified using a Multiclamp 700B amplifier (Molecular Devices) and digitised using the Digidata 1440 (Molecular Devices). Data were recorded (pClamp 10.2, Molecular Devices) for offline analysis. The magnitude of LTP was quantified by normalising and averaging the slope of fEPSPs following LTP induction relative to the last 5 min of baseline.

## Two-photon calcium imaging and analysis

Fluorescence calcium imaging was performed on a custom two-photon laser-scanning microscope (Scientifica). The microscope was equipped with a Ti:Sapph laser (Ultra II, Coherent), a green band-pass emission filter (525–40 nm), an orange/red bandpass emission filter (605–70 nm), and associated photomultiplier tubes (GaAsP, Hamamatsu). Time-series images were acquired through bidirectional laser scanning (920 nm excitation laser, 86.85 µm × 86.85 µm, 512 × 512 pixels at 1 Hz) at a single

focal plane incorporating the entirety of the imaged astrocyte ramifications. All images were acquired using Scanimage (MBF Bioscience). Acute brain slices (350  $\mu\text{m}$ ) containing the lateral amygdala were obtained from mice (ages between P45 and 70) injected with the viral construct AAV2/5-gfaABC1D-lck-GCaMP6f 3 weeks prior. Animals were anaesthetised with isoflurane and the brain was rapidly excised and placed in ice-cold NMDG-based cutting solution saturated with 95%  $\text{O}_2$  and 5%  $\text{CO}_2$  containing the following (in mM): 119.9 NMDG, 2.5 KCl, 25, 1  $\text{CaCl}_2$ , 1.4  $\text{NaH}_2\text{PO}_4$ , and 20 D-glucose saturated with 95%  $\text{O}_2$  and 5%  $\text{CO}_2$ . Slices (350  $\mu\text{m}$  thick) were cut on a vibratome (Leica VT1200, Nussloch, Germany). Slices were transferred to oxygenated NMDG cutting solution ACSF at  $33 \pm 0.5^\circ\text{C}$  for 15 min followed by a 1 hr recovery period in ACSF at RT containing the following (in mM): 130 NaCl, 2.5 KCl, 1.25  $\text{NaH}_2\text{PO}_4$ , 26  $\text{NaHCO}_3$ , 2.5 glucose, 1.3  $\text{MgCl}_2$ , 2  $\text{CaCl}_2$ , pH 7.3–7.4, and 300–305 mOsmol. All time-series images were acquired in a recording chamber constantly perfused with ACSF as described above.

For unbiased, automatic calcium event detection, TIFF files of time-lapse images were processed with the AQUA2 pipeline in MATLAB. Parameters of interest (event frequency, amplitude, area, duration, rise time, and decay time) were directly extracted from the AQUA2 output file. For statistical testing, averages of all events from a single astrocyte were calculated for each parameter. In parallel, to better represent the diversity in calcium events, frequency distributions plots were created considering every detected event for all our experimental conditions.

### Stereotaxic surgery and AAV delivery

P25–35 mice were given a subcutaneous (sc) injection of carprofen (20 mg/kg) 1 hr prior surgery. Animals were then deeply anaesthetised (2% isoflurane) before placing them into a stereotaxic frame (Kopf Instruments). Surgical site was infiltrated with bupivacaine/lidocaine (2 mg/kg sc) 15 min prior surgery. Bilateral injections of the following viral constructs produced at the Canadian Neurophotonics Viral Vector Core: AAV2/5-gfaABC1D-lck-GCaMP6f ( $9.6 \times 10^{12}$  GC/ml), AAV2/5-gfaABC1D-eGFP ( $1.2\text{--}1.5 \times 10^{11\text{--}12}$  GC/ml), AAV2/5-gfaABC1D-dnCx43-eGFP ( $1.2\text{--}1.7 \times 10^{12}$  GC/ml), and AAV2/5-gfaABC1D-hPMCAw/b-mCherry ( $1.2 \times 10^{12}$ ) were delivered to the LA (coordinates relative to bregma:  $-1.4$  mm AP,  $\pm 3.4$  mm ML and  $-5$  mm DV) of mice of either sex. Viral solutions were injected at a rate of 200 nl/min for a total volume of 650 nl per hemisphere using a 10  $\mu\text{l}$  Hamilton syringe (Harvard apparatus) and a microinjection syringe pump (UMP3T-2 World Precision Instruments). Animals received 250  $\mu\text{l}$  of saline for post-surgery hydration.

### Brain processing

Mice were anaesthetised in an enclosed chamber filled with isoflurane (5% for induction, 3–4% for maintenance, v/v) until loss of toe pinch reflex. A transcardial perfusion was used to ensure uniform preservation of tissue and brains were fixed in 4% paraformaldehyde for 24 hr at  $4^\circ\text{C}$ . The fixed brains were then placed in falcon tubes containing 30% sucrose solution for a minimum of 2 days. Brains were embedded in optimal cutting temperature compound and flash frozen in 2-methylbutane between  $-40$  and  $-50^\circ\text{C}$  and then stored at  $-80$  until cryosectioning. Brains were cut at 30  $\mu\text{m}$  thickness at  $-20^\circ\text{C}$  using a Leica CM3050S Cryostat. Slices were stored in cryoprotector solution at  $4^\circ\text{C}$  until immunohistochemistry.

For c-Fos labelling experiments, mice were anaesthetised and then perfused 90 min after the end of fear conditioning. The whole lateral amygdala was sectioned in 30- $\mu\text{m}$ -thick brain slices, and every fourth brain slice was selected for immunohistochemistry.

### Immunohistochemistry

Free-floating brain slices were washed three times in  $1 \times$  PBS for 15 min to remove cryoprotector solution. Slices were permeabilised in block-perm solution (3% bovine serum albumin, 0.5% Triton<sup>10%</sup> in PBS) for a duration of 1 hr. Slices were incubated with antibodies for 24 hr at  $4^\circ\text{C}$ . Slices were incubated with primary antibodies; [rabbit] anti-S100 $\beta$  (1:1000, Abcam, ab52642), [mouse] anti-GR (1:500, Thermo Fisher, MA1-510), [chicken] anti-GFAP (1:1000, Thermo Fisher, PA1-10004), [mouse] anti-Cx43 (1:1000 Thermo Fisher, 3D8A5), [rabbit] anti-GLT-1 (EAAT2) (1:1000, NovusBio, NBP1-20136), and [rabbit] anti-c-Fos (1:2000, Synaptic Systems, Cat# 226008). After primary antibody incubation, slices were washed three times in  $1 \times$  PBS for 15 min to remove non-specific binding. Slices were incubated with secondary antibodies in a DAPI solution (1:10,000) at RT in aluminium foil for 1 hr. Slices were



incubated with secondary antibodies; [goat] anti-rabbit Alexa 488 (1:1000, Jackson ImmunoResearch, 111-545-144), [goat] anti-mouse Alexa 647 (1:1000, Thermo Fisher, A32728), and [goat] anti-chicken Alexa 568 (1:1000, Thermo Fisher, A11041). After secondary antibody incubation, slices were washed again three times in 1× PBS for 15 min before being mounted onto Fisherbrand microscope slides using ProLong Glass Antifade mountant (P36982).

## Microscopy

Slices were imaged using a Leica TCS SP5 laser scanning confocal microscope with oil immersion Plan-Apochromat ×63 objective 1.4 NA or using a Zeiss Observer Z1 spinning disk confocal microscope/TIRF with a ×20 objective 1.8 NA. 16-bit images of 246 × 246 μm areas were acquired at 400 Hz (frame size (x\*y); 1024 × 1024, pixel size; 250 nm). 25–30 μm Z-stacks were acquired with a step size of 0.5 μm. 15 μm max intensity z-projections of the lateral amygdala were analysed using ImageJ (Fiji) to obtain A.U. fluorescence intensity measures of secondary antibodies attached to primaries with specificity to epitopes; GFAP, Cx43, GLT-1, and GR. We applied a fluorescence threshold for GFAP, Cx43, and GLT-1 fluorescence and measured integrated density A.U. (thresholds; Mean, Otsu, Otsu, respectively). For nuclear and cytosolic GR measures, astrocyte (S100β+DAPI) nuclei were thresholded and used as regions of interest (ROIs) for nuclear measures of GR fluorescence (S100β<sup>+</sup> + DAPI<sup>+</sup>). The same nuclear DAPI ROI was cleared from the previously thresholded s100b regions to obtain cytosolic astrocytic GR (S100β<sup>+</sup> - DAPI<sup>+</sup>). Integrated density A.U. of GR fluorescence was used to calculate nuclear:cytosolic GR ratios.

For c-Fos cell counting in the lateral amygdala, 16-bit images containing the lateral and basal amygdala nuclei were acquired. 20–30 Z-stacks were acquired with a step size of 1 μm. For c-Fos particle counting analysis, a ROI was used to isolate the lateral amygdala and then 8-bit Z-stacks of the c-Fos channel were analysed semi-automatically by using the FIJI plugin Quanty-cfos (Beretta *et al.*, 2023). In brief, a threshold for area and fluorescence intensity was set manually to identify ROIs around all c-Fos-positive nuclei. These ROIs were then manually inspected to remove false positives and negatives found by the plug-in. c-Fos particle counts were then normalised by the volume of the Z-stack to calculate the c-Fos density. In order to calculate the volume, the area of the lateral amygdala was multiplied by the number of Z-stacks.

## Blood collection and corticosterone analysis

Trunk blood was collected via decapitation at ZT2 (08:30). To minimise handling-induced elevations in corticosterone, mice were housed with clear plastic tubes used to move individual mice into an enclosed chamber filled with 5% isoflurane for 2 min. Mice were placed in enclosed isoflurane until loss of toe pinch reflect (maximum elapsed time of 2 min). Mice were decapitated and trunk blood was collected into BD 365963 Microtainer Capillary Blood Collection Tubes and placed onto ice. Blood was centrifuged for 5 min at 4°C at 5000 rpm. Serum was aliquoted and stored at –80°C. Corticosterone measurements were obtained using an ENZO ELISA kit (ADI-900-097).

## Statistical analyses

Detailed statistical analyses are provided in **Supplementary file 1**. Results are presented as mean ± SEM. Data with one variable were analysed with the two-tailed Student's *t*-test or Mann–Whitney test. Data with more than two conditions were first screened for a Gaussian distribution with Kolmogorov–Smirnov test followed by analysis either with one-way/repeated-measures ANOVA or Kruskal–Wallis/Friedman test when needed and Tukey's multiple-comparison parametric *post hoc* test (data with Gaussian distribution) or by a Dunn's multiple-comparison non-parametric *post hoc* test (data with non-Gaussian distribution). Auditory discriminative fear conditioning data was analysed using a two-way ANOVA with appropriate *post hoc* tests. Open-field and elevated plus maze data was analysed using one-way ANOVA with appropriate *post hoc* tests. Graphic significance levels were \**p*<0.05; \*\**p*<0.01, and \*\*\**p*<0.001. All data were analysed using GraphPad Prism software (version 9, GraphPad, USA).

## Acknowledgements

We thank Rosemary Bagot (McGill University) for critical input on this study, Thierry Alquier and Stephanie Fulton (Université de Montréal) for their input throughout, Aurélie Cleret-Buhot (CRCHUM cellular imaging core) for microscopy training, and the staff of the animal facility at the CRCHUM. This work was funded by the Canadian Institutes of Health Research Project Grant (478629), NSERC Discovery Grant (RGPIN-2021-03211), Fonds de Recherche du Québec – Santé (FRQS; 296562 and 309889), Brain and Behaviour Research Foundation Young Investigator award (NARSAD; 28589), CHUM Foundation, Fondation Courtois, and the Réseau Québécois sur le Suicide les troubles de l’humeur et les troubles Associées (RQSHA) grant to CM-R. LD-H was supported by a doctoral fellowship from the Fonds de Recherche du Québec. IIA, JV, and BR were supported by a Canada Graduate Scholarship Master’s award, and Recruitment Fellowships from Neuroscience Dept. Université de Montréal. CM-R was supported by a Junior 1 Chercheur-Boursier salary award from FRQS.

## Additional information

### Funding




Funder	Grant reference number	Author
Canadian Institutes of Health Research	478629	Ciaran Murphy-Royal
Natural Sciences and Engineering Research Council of Canada	RGPIN-2021-03211	Ciaran Murphy-Royal
Fonds de Recherche du Québec - Santé	296562	Ciaran Murphy-Royal
Fonds de Recherche du Québec - Santé	309889	Ciaran Murphy-Royal
Fondation du CHUM		Ciaran Murphy-Royal
Fondation Courtois		Ciaran Murphy-Royal
Réseau Québécois sur le Suicide, les troubles de l’humeur, et les troubles associées		Ciaran Murphy-Royal
Fonds de Recherche du Québec - Santé	Doctoral Scholarship	Lewis R Depaauw-Holt
Canadian Institutes of Health Research	Master's Scholarships	Ifeoluwa I Adedipe Juliette Vaugeois Benjamin Rogers
Brain and Behavior Research Foundation	Young Investigator NARSAD; 28589	Ciaran Murphy-Royal

The funders had no role in study design, data collection and interpretation, or the decision to submit the work for publication.

### Author contributions

Mathias Guayasamin, Lewis R Depaauw-Holt, Conceptualization, Data curation, Formal analysis, Validation, Investigation, Methodology, Writing – original draft, Writing – review and editing; Ifeoluwa I Adedipe, Conceptualization, Data curation, Formal analysis, Investigation, Methodology, Writing – original draft; Ossama Ghenissa, Data curation, Formal analysis, Writing – review and editing; Juliette Vaugeois, Manon Duquenne, Data curation, Formal analysis; Benjamin Rogers, Jade Latraverse-Arquilla, Data curation; Sarah Peyrard, Resources, Methodology, Project administration; Anthony Bosson, Conceptualization, Data curation, Formal analysis, Writing – original draft, Writing – review and editing; Ciaran Murphy-Royal, Conceptualization, Resources, Data curation, Formal analysis, Supervision, Funding acquisition, Validation, Investigation, Methodology, Writing – original draft, Project administration, Writing – review and editing

**Author ORCIDs**

Mathias Guayasamin  <https://orcid.org/0009-0008-6099-930X>  
 Lewis R Depaauw-Holt  <https://orcid.org/0009-0001-3797-447X>  
 Ciaran Murphy-Royal  <https://orcid.org/0000-0001-7545-593X>

**Ethics**

All experiments were performed in accordance with the guidelines for maintenance and care of animals of the Canadian Council on Animal Care (CCAC) and approved by the Institutional Committee for the Protection of Animals (CIPA) at the Centre Hospitalier de de l'Université de Montréal. protocol number CM20031CMRs.

**Peer review material**

Reviewer #1 (Public review): <https://doi.org/10.7554/eLife.99988.3.sa1>

Reviewer #2 (Public review): <https://doi.org/10.7554/eLife.99988.3.sa2>

Reviewer #3 (Public review): <https://doi.org/10.7554/eLife.99988.3.sa3>

Author response <https://doi.org/10.7554/eLife.99988.3.sa4>

**Additional files****Supplementary files**

MDAR checklist

Supplementary file 1. Document containing detailed statistical tests used in each figure.

**Data availability**

Source data is available on the Open Science Framework.

The following dataset was generated:

Author(s)	Year	Dataset title	Dataset URL	Database and Identifier
Murphy-Royal C	2025	Guayasamin et al. eLife manuscript data	<a href="https://osf.io/zsw6j/">https://osf.io/zsw6j/</a>	Open Science Framework, 10.17605/OSF.IO/ZSW6J

**References**

- Abbink MR**, van Deijk A-LF, Heine VM, Verheijen MH, Korosi A. 2019. The involvement of astrocytes in early-life adversity induced programming of the brain. *GLIA* **67**:1637–1653. DOI: <https://doi.org/10.1002/glia.23625>, PMID: 31038797
- Adamsky A**, Kol A, Kreisel T, Doron A, Ozeri-Engelhard N, Melcer T, Refaeli R, Horn H, Regev L, Groysman M, London M, Goshen I. 2018. Astrocytic activation generates de novo neuronal potentiation and memory enhancement. *Cell* **174**:59–71. DOI: <https://doi.org/10.1016/j.cell.2018.05.002>, PMID: 29804835
- Asok A**, Kandel ER, Rayman JB. 2018. The neurobiology of fear generalization. *Frontiers in Behavioral Neuroscience* **12**:329. DOI: <https://doi.org/10.3389/fnbeh.2018.00329>, PMID: 30697153
- Bains JS**, Wamsteeker Cusulin JI, Inoue W. 2015. Stress-related synaptic plasticity in the hypothalamus. *Nature Reviews. Neuroscience* **16**:377–388. DOI: <https://doi.org/10.1038/nrn3881>, PMID: 26087679
- Balouek J-A**, Mclain CA, Minerva AR, Rashford RL, Bennett SN, Rogers FD, Peña CJ. 2023. Reactivation of Early-Life Stress-Sensitive Neuronal Ensembles Contributes to Lifelong Stress Hypersensitivity. *The Journal of Neuroscience* **43**:5996–6009. DOI: <https://doi.org/10.1523/JNEUROSCI.0016-23.2023>, PMID: 37429717
- Beretta CA**, Liu S, Stegemann A, Gan Z, Wang L, Tan LL, Kuner R. 2023. Quanty-cFOS, a Novel ImageJ/Fiji algorithm for automated counting of immunoreactive cells in tissue sections. *Cells* **12**:704. DOI: <https://doi.org/10.3390/cells12050704>, PMID: 36899840
- Chen AB**, Duque M, Wang VM, Dhanasekar M, Mi X, Rymbek A, Tocquer L, Narayan S, Prober D, Yu G, Wyart C, Engert F, Ahrens MB. 2024. Norepinephrine changes behavioral state via astroglial purinergic signaling. *bioRxiv*. DOI: <https://doi.org/10.1101/2024.05.23.595576>
- Covelo A**, Araque A. 2018. Neuronal activity determines distinct gliotransmitter release from a single astrocyte. *eLife* **7**:e32237. DOI: <https://doi.org/10.7554/eLife.32237>, PMID: 29380725
- Daviu N**, Füzesi T, Rosenegger DG, Rasiyah NP, Sterley TL, Peringod G, Bains JS. 2020. Paraventricular nucleus CRH neurons encode stress controllability and regulate defensive behavior selection. *Nature Neuroscience* **23**:398–410. DOI: <https://doi.org/10.1038/s41593-020-0591-0>, PMID: 32066984
- de Kloet ER**, Joëls M, Holsboer F. 2005. Stress and the brain: from adaptation to disease. *Nature Reviews. Neuroscience* **6**:463–475. DOI: <https://doi.org/10.1038/nrn1683>, PMID: 15891777

- Depaauw-Holt LR**, Hamane S, Peyrard S, Rogers B, Fulton S, Bosson A, Murphy-Royal C. 2024. Astrocyte glucocorticoid receptors mediate sex-specific changes in activity following stress. *bioRxiv*. DOI: <https://doi.org/10.1101/2024.09.17.613499>
- Doron A**, Rubin A, Benmelech-Chovav A, Benaim N, Carmi T, Refaeli R, Novick N, Kreisel T, Ziv Y, Goshen I. 2022. Hippocampal astrocytes encode reward location. *Nature* **609**:772–778. DOI: <https://doi.org/10.1038/s41586-022-05146-6>, PMID: 36045289
- Dymond S**, Dunsmoor JE, Vervliet B, Roche B, Hermans D. 2015. Fear generalization in humans. *Systematic Review and Implications for Anxiety Disorder Research. Behav Ther* **46**:561–582. DOI: <https://doi.org/10.1016/j.beth.2014.10.001>
- Elliott ND**, Richardson R. 2019. The effects of early life stress on context fear generalization in adult rats. *Behavioral Neuroscience* **133**:50–58. DOI: <https://doi.org/10.1037/bne0000289>, PMID: 30489134
- Endo F**, Kasai A, Soto JS, Yu X, Qu Z, Hashimoto H, Gradinaru V, Kawaguchi R, Khakh BS. 2022. Molecular basis of astrocyte diversity and morphology across the CNS in health and disease. *Science* **378**:eadc9020. DOI: <https://doi.org/10.1126/science.adc9020>, PMID: 36378959
- Farhy Tselnicker I**, Allen NJ. 2018. Astrocytes, neurons, synapses: a tripartite view on cortical circuit development. *Neural Development* **13**:7. DOI: <https://doi.org/10.1186/s13064-018-0104-y>, PMID: 29712572
- Füzesi T**, Daviu N, Wamsteeker Cusulin JI, Bonin RP, Bains JS. 2016. Hypothalamic CRH neurons orchestrate complex behaviours after stress. *Nature Communications* **7**:11937. DOI: <https://doi.org/10.1038/ncomms11937>, PMID: 27306314
- Giaume C**, Koulakoff A, Roux L, Holcman D, Rouach N. 2010. Astroglial networks: a step further in neuroglial and gliovascular interactions. *Nature Reviews. Neuroscience* **11**:87–99. DOI: <https://doi.org/10.1038/nrn2757>, PMID: 20087359
- González-Vila A**, Luengo-Mateos M, Silveira-Loureiro M, Garrido-Gil P, Ohinska N, González-Domínguez M, Labandeira-García JL, García-Cáceres C, López M, Barca-Mayo O. 2023. Astrocytic insulin receptor controls circadian behavior via dopamine signaling in a sexually dimorphic manner. *Nature Communications* **14**:8175. DOI: <https://doi.org/10.1038/s41467-023-44039-8>, PMID: 38071352
- Guadagno A**, Kang MS, Devenyi GA, Mathieu AP, Rosa-Neto P, Chakravarty M, Walker CD. 2018a. Reduced resting-state functional connectivity of the basolateral amygdala to the medial prefrontal cortex in preweaning rats exposed to chronic early-life stress. *Brain Structure & Function* **223**:3711–3729. DOI: <https://doi.org/10.1007/s00429-018-1720-3>, PMID: 30032360
- Guadagno A**, Wong TP, Walker CD. 2018b. Morphological and functional changes in the preweaning basolateral amygdala induced by early chronic stress associate with anxiety and fear behavior in adult male, but not female rats. *Progress in Neuro-Psychopharmacology & Biological Psychiatry* **81**:25–37. DOI: <https://doi.org/10.1016/j.pnpbp.2017.09.025>, PMID: 28963066
- Guadagno A**, Belliveau C, Mechawar N, Walker CD. 2021. Effects of early life stress on the developing basolateral amygdala-prefrontal cortex circuit: the emerging role of local inhibition and perineuronal nets. *Frontiers in Human Neuroscience* **15**:669120. DOI: <https://doi.org/10.3389/fnhum.2021.669120>, PMID: 34512291
- Gunn BG**, Cunningham L, Cooper MA, Corteen NL, Seifi M, Swinny JD, Lambert JJ, Belelli D. 2013. Dysfunctional astrocytic and synaptic regulation of hypothalamic glutamatergic transmission in a mouse model of early-life adversity: relevance to neurosteroids and programming of the stress response. *The Journal of Neuroscience* **33**:19534–19554. DOI: <https://doi.org/10.1523/JNEUROSCI.1337-13.2013>, PMID: 24336719
- Guttenplan KA**, Maxwell I, Santos E, Borchardt LA, Manzo E, Abalde-Atristain L, Kim RD, Freeman MR. 2024. Adrenergic Signaling Gates Astrocyte Responsiveness to Neurotransmitters and Control of Neuronal Activity. *bioRxiv*. DOI: <https://doi.org/10.1101/2024.09.23.614537>
- Henneberger C**, Papouin T, Oliet SHR, Rusakov DA. 2010. Long-term potentiation depends on release of D-serine from astrocytes. *Nature* **463**:232–236. DOI: <https://doi.org/10.1038/nature08673>, PMID: 20075918
- Institoris A**, Vandal M, Peringod G, Catalano C, Tran CH, Yu X, Visser F, Breiteneder C, Molina L, Khakh BS, Nguyen MD, Thompson RJ, Gordon GR. 2022. Astrocytes amplify neurovascular coupling to sustained activation of neocortex in awake mice. *Nature Communications* **13**:7872. DOI: <https://doi.org/10.1038/s41467-022-35383-2>, PMID: 36550102
- Joëls M**, Baram TZ. 2009. The neuro-symphony of stress. *Nature Reviews. Neuroscience* **10**:459–466. DOI: <https://doi.org/10.1038/nrn2632>, PMID: 19339973
- Josselyn SA**, Köhler S, Frankland PW. 2015. Finding the engram. *Nature Reviews. Neuroscience* **16**:521–534. DOI: <https://doi.org/10.1038/nrn4000>, PMID: 26289572
- Khakh BS**, Goldman SA. 2023. Astrocytic contributions to Huntington's disease pathophysiology. *Annals of the New York Academy of Sciences* **1522**:42–59. DOI: <https://doi.org/10.1111/nyas.14977>, PMID: 36864567
- Kim WB**, Cho J-H. 2017. Encoding of discriminative fear memory by input-specific LTP in the amygdala. *Neuron* **95**:1129–1146. DOI: <https://doi.org/10.1016/j.neuron.2017.08.004>
- Kim J**, Sung Y, Park H, Choi DI, Kim J, Lee H, Jung MK, Noh S, Ye S, Lee J, Islam MA, Chun H, Mun JY, Kaang BK. 2023. Astrocytic Connection to Engram Neurons Increased after Learning. *bioRxiv*. DOI: <https://doi.org/10.1101/2023.01.25.525617>
- Kol A**, Adamsky A, Groysman M, Kreisel T, London M, Goshen I. 2020. Astrocytes contribute to remote memory formation by modulating hippocampal-cortical communication during learning. *Nature Neuroscience* **23**:1229–1239. DOI: <https://doi.org/10.1038/s41593-020-0679-6>, PMID: 32747787

- Kruyer A**, Scofield MD, Wood D, Reissner KJ, Kalivas PW. 2019. Heroin cue-evoked astrocytic structural plasticity at nucleus accumbens synapses inhibits heroin seeking. *Biological Psychiatry* **86**:811–819. DOI: <https://doi.org/10.1016/j.biopsych.2019.06.026>, PMID: 31495448
- Kruyer A**, Angelis A, Garcia-Keller C, Li H, Kalivas PW. 2022. Plasticity in astrocyte subpopulations regulates heroin relapse. *Science Advances* **8**:eabo7044. DOI: <https://doi.org/10.1126/sciadv.abo7044>, PMID: 35947652
- Lau BK**, Murphy-Royal C, Kaur M, Qiao M, Bains JS, Gordon GR, Borgland SL. 2021. Obesity-induced astrocyte dysfunction impairs heterosynaptic plasticity in the orbitofrontal cortex. *Cell Reports* **36**:109563. DOI: <https://doi.org/10.1016/j.celrep.2021.109563>, PMID: 34407401
- Lee HG**, Wheeler MA, Quintana FJ. 2022. Function and therapeutic value of astrocytes in neurological diseases. *Nature Reviews. Drug Discovery* **21**:339–358. DOI: <https://doi.org/10.1038/s41573-022-00390-x>, PMID: 35173313
- Lefton KB**, Wu Y, Yen A, Okuda T, Zhang Y, Dai Y, Walsh S, Manno R, Dougherty JD, Samineni VK, Simpson PC, Papouin T. 2024. Norepinephrine Signals through Astrocytes to Modulate Synapses. *bioRxiv*. DOI: <https://doi.org/10.1101/2024.05.21.595135>
- Lesuis SL**, Weggen S, Baches S, Lucassen PJ, Krugers HJ. 2018. Targeting glucocorticoid receptors prevents the effects of early life stress on amyloid pathology and cognitive performance in APP/PS1 mice. *Translational Psychiatry* **8**:53. DOI: <https://doi.org/10.1038/s41398-018-0101-2>, PMID: 29491368
- Lesuis SL**, Lucassen PJ, Krugers HJ. 2019. Early life stress impairs fear memory and synaptic plasticity; a potential role for GluN2B. *Neuropharmacology* **149**:195–203. DOI: <https://doi.org/10.1016/j.neuropharm.2019.01.010>, PMID: 30641077
- Lesuis SL**, Brosens N, Immerzeel N, van der Loo RJ, Mitrić M, Bielefeld P, Fitzsimons CP, Lucassen PJ, Kushner SA, van den Oever MC, Krugers HJ. 2021. Glucocorticoids promote fear generalization by increasing the size of a dentate gyrus engram cell population. *Biological Psychiatry* **90**:494–504. DOI: <https://doi.org/10.1016/j.biopsych.2021.04.010>, PMID: 34503674
- Lesuis SL**, Park S, Hoorn A, Rashid AJ, Mocle AJ, Salter EW, Vislavski S, Gray MT, Torelli AM, DeCristofaro A, Driever WPF, van der Stelt M, Zweifel LS, Collingridge GL, Lefebvre JL, Walters BJ, Frankland PW, Hill MN, Josselyn SA. 2025. Stress disrupts engram ensembles in lateral amygdala to generalize threat memory in mice. *Cell* **188**:121–140. DOI: <https://doi.org/10.1016/j.cell.2024.10.034>, PMID: 39549697
- Lis S**, Thome J, Kleindienst N, Mueller-Engelmann M, Steil R, Priebe K, Schmahl C, Hermans D, Bohus M. 2020. Generalization of fear in post-traumatic stress disorder. *Psychophysiology* **57**:e13422. DOI: <https://doi.org/10.1111/psyp.13422>, PMID: 31206738
- Lissek S**, van Meurs B. 2015. Learning models of PTSD: Theoretical accounts and psychobiological evidence. *International Journal of Psychophysiology* **98**:594–605. DOI: <https://doi.org/10.1016/j.ijpsycho.2014.11.006>, PMID: 25462219
- Lopez J**, Bagot RC. 2021. Defining valid chronic stress models for depression with female rodents. *Biological Psychiatry* **90**:226–235. DOI: <https://doi.org/10.1016/j.biopsych.2021.03.010>, PMID: 33965195
- Lupien SJ**, McEwen BS, Gunnar MR, Heim C. 2009. Effects of stress throughout the lifespan on the brain, behaviour and cognition. *Nature Reviews. Neuroscience* **10**:434–445. DOI: <https://doi.org/10.1038/nrn2639>, PMID: 19401723
- Malter Cohen M**, Jing D, Yang RR, Tottenham N, Lee FS, Casey BJ. 2013. Early-life stress has persistent effects on amygdala function and development in mice and humans. *PNAS* **110**:18274–18278. DOI: <https://doi.org/10.1073/pnas.1310163110>
- Martin-Fernandez M**, Jamison S, Robin LM, Zhao Z, Martin ED, Aguilar J, Benneyworth MA, Marsicano G, Araque A. 2017. Synapse-specific astrocyte gating of amygdala-related behavior. *Nature Neuroscience* **20**:1540–1548. DOI: <https://doi.org/10.1038/nn.4649>, PMID: 28945222
- Matos M**, Bosson A, Riebe I, Reynell C, Vallée J, Laplante I, Panatier A, Robitaille R, Lacaille J-C. 2018. Astrocytes detect and upregulate transmission at inhibitory synapses of somatostatin interneurons onto pyramidal cells. *Nature Communications* **9**:4254. DOI: <https://doi.org/10.1038/s41467-018-06731-y>, PMID: 30315174
- Meaney MJ**. 2001. Maternal care, gene expression, and the transmission of individual differences in stress reactivity across generations. *Annual Review of Neuroscience* **24**:1161–1192. DOI: <https://doi.org/10.1146/annurev.neuro.24.1.1161>, PMID: 11520931
- Mi X**, Chen ABY, Duarte D, Carey E, Taylor CR, Braaker PN, Bright M, Almeida RG, Lim JX, Ruetten VMS, Zheng W, Wang M, Reitman ME, Wang Y, Poskanzer KE, Lyons DA, Nimmerjahn A, Ahrens MB, Yu G. 2024. Fast, Accurate, and Versatile Data Analysis Platform for the Quantification of Molecular Spatiotemporal Signals. *bioRxiv*. DOI: <https://doi.org/10.1101/2024.05.02.592259>
- Mu Y**, Bennett DV, Rubinov M, Narayan S, Yang C-T, Tanimoto M, Mensh BD, Looger LL, Ahrens MB. 2019. Glia accumulate evidence that actions are futile and suppress unsuccessful behavior. *Cell* **178**:27–43. DOI: <https://doi.org/10.1016/j.cell.2019.05.050>, PMID: 31230713
- Murphy-Royal C**, Dupuis JP, Varela JA, Panatier A, Pinson B, Baufreton J, Groc L, Oliet SHR. 2015. Surface diffusion of astrocytic glutamate transporters shapes synaptic transmission. *Nature Neuroscience* **18**:219–226. DOI: <https://doi.org/10.1038/nn.3901>, PMID: 25581361
- Murphy-Royal C**, Johnston AD, Boyce AKJ, Diaz-Castro B, Institoris A, Peringod G, Zhang O, Stout RF, Spray DC, Thompson RJ, Khakh BS, Bains JS, Gordon GR. 2020. Stress gates an astrocytic energy reservoir to impair synaptic plasticity. *Nature Communications* **11**:2014. DOI: <https://doi.org/10.1038/s41467-020-15778-9>, PMID: 32332733

- Murphy-Royal C**, Ching SN, Papouin T. 2023. A conceptual framework for astrocyte function. *Nature Neuroscience* **26**:1848–1856. DOI: <https://doi.org/10.1038/s41593-023-01448-8>, PMID: 37857773
- Nagai J**, Rajbhandari AK, Gangwani MR, Hachisuka A, Coppola G, Masmanidis SC, Fanselow MS, Khakh BS. 2019. Hyperactivity with disrupted attention by activation of an astrocyte synaptogenic cue. *Cell* **177**:1280–1292. DOI: <https://doi.org/10.1016/j.cell.2019.03.019>, PMID: 31031006
- Nagai J**, Yu X, Papouin T, Cheong E, Freeman MR, Monk KR, Hastings MH, Haydon PG, Rowitch D, Shaham S, Khakh BS. 2021. Behaviorally consequential astrocytic regulation of neural circuits. *Neuron* **109**:576–596. DOI: <https://doi.org/10.1016/j.neuron.2020.12.008>, PMID: 33385325
- O'Donnell KJ**, Meaney MJ. 2020. Epigenetics, development, and psychopathology. *Annual Review of Clinical Psychology* **16**:327–350. DOI: <https://doi.org/10.1146/annurev-clinpsy-050718-095530>, PMID: 32084320
- Panatier A**, Theodosis DT, Mothet JP, Touquet B, Pollegioni L, Poulain DA, Oliet SHR. 2006. Glia-derived D-serine controls NMDA receptor activity and synaptic memory. *Cell* **125**:775–784. DOI: <https://doi.org/10.1016/j.cell.2006.02.051>, PMID: 16713567
- Panatier A**, Vallée J, Haber M, Murai KK, Lacaille JC, Robitaille R. 2011. Astrocytes are endogenous regulators of basal transmission at central synapses. *Cell* **146**:785–798. DOI: <https://doi.org/10.1016/j.cell.2011.07.022>, PMID: 21855979
- Papouin T**, Dunphy JM, Tolman M, Dineley KT, Haydon PG. 2017. Septal cholinergic neuromodulation tunes the astrocyte-dependent gating of hippocampal nmda receptors to wakefulness. *Neuron* **94**:840–854. DOI: <https://doi.org/10.1016/j.neuron.2017.04.021>, PMID: 28479102
- Peña CJ**, Kronman HG, Walker DM, Cates HM, Bagot RC, Purushothaman I, Issler O, Loh Y-HE, Leong T, Kiraly DD, Goodman E, Neve RL, Shen L, Nestler EJ. 2017. Early life stress confers lifelong stress susceptibility in mice via ventral tegmental area OTX2. *Science* **356**:1185–1188. DOI: <https://doi.org/10.1126/science.aan4491>, PMID: 28619944
- Peña CJ**, Nestler EJ, Bagot RC. 2019. Environmental programming of susceptibility and resilience to stress in adulthood in male mice. *Frontiers in Behavioral Neuroscience* **13**:40. DOI: <https://doi.org/10.3389/fnbeh.2019.00040>, PMID: 30881296
- Ramkumar R**, Edge-Partington M, Terstege DJ, Adigun K, Ren Y, Khan NS, Rouhi N, Jamani NF, Tsutsui M, Epp JR, Sargin D. 2024. Long-term impact of early-life stress on serotonin connectivity. *Biological Psychiatry* **96**:287–299. DOI: <https://doi.org/10.1016/j.biopsych.2024.01.024>, PMID: 38316332
- Ramsaran AI**, Wang Y, Golbabaie A, Aleshin S, de Snoo ML, Yeung B-RA, Rashid AJ, Awasthi A, Lau J, Tran LM, Ko SY, Abegg A, Duan LC, McKenzie C, Gallucci J, Ahmed M, Kaushik R, Dityatev A, Josselyn SA, Frankland PW. 2023. A shift in the mechanisms controlling hippocampal engram formation during brain maturation. *Science* **380**:543–551. DOI: <https://doi.org/10.1126/science.ade6530>, PMID: 37141366
- Ramsaran AI**, Ventura S, Gallucci J, De Snoo ML, Josselyn SA, Frankland PW. 2024. A Sensitive Period for the Development of Episodic-like Memory in Mice. *bioRxiv*. DOI: <https://doi.org/10.1101/2024.11.06.622296>, PMID: 39574753
- Rashid AJ**, Yan C, Mercaldo V, Hsiang H-LL, Park S, Cole CJ, De Cristofaro A, Yu J, Ramakrishnan C, Lee SY, Deisseroth K, Frankland PW, Josselyn SA. 2016. Competition between engrams influences fear memory formation and recall. *Science* **353**:383–387. DOI: <https://doi.org/10.1126/science.aaf0594>, PMID: 27463673
- Ressler KJ**. 2010. Amygdala activity, fear, and anxiety: modulation by stress. *Biological Psychiatry* **67**:1117–1119. DOI: <https://doi.org/10.1016/j.biopsych.2010.04.027>, PMID: 20525501
- Robin LM**, Oliveira da Cruz JF, Langlais VC, Martin-Fernandez M, Metna-Laurent M, Busquets-Garcia A, Bellocchio L, Soria-Gomez E, Papouin T, Varilh M, Sherwood MW, Belluomo I, Balcells G, Matias I, Bosier B, Drago F, Van Eeckhout A, Smolders I, Georges F, Araque A, et al. 2018. Astroglial CB<sub>1</sub> receptors determine synaptic d-serine availability to enable recognition memory. *Neuron* **98**:935–944. DOI: <https://doi.org/10.1016/j.neuron.2018.04.034>, PMID: 29779943
- Roosendaal B**, McEwen BS, Chattarji S. 2009. Stress, memory and the amygdala. *Nature Reviews. Neuroscience* **10**:423–433. DOI: <https://doi.org/10.1038/nrn2651>, PMID: 19469026
- Rurak GM**, Simard S, Freitas-Andrade M, Lacoste B, Charif F, Van Geel A, Stead J, Woodside B, Green JR, Coppola G, Salmasso N. 2022. Sex differences in developmental patterns of neocortical astroglia: a mouse transcriptome database. *Cell Reports* **38**:110310. DOI: <https://doi.org/10.1016/j.celrep.2022.110310>, PMID: 35108542
- Sapolsky RM**, Meaney MJ. 1986. Maturation of the adrenocortical stress response: neuroendocrine control mechanisms and the stress hyporesponsive period. *Brain Research* **396**:64–76. DOI: [https://doi.org/10.1016/s0006-8993\(86\)80190-1](https://doi.org/10.1016/s0006-8993(86)80190-1), PMID: 3011218
- Schmidt MV**, Enthoven L, van der Mark M, Levine S, de Kloet ER, Oitzl MS. 2003. The postnatal development of the hypothalamic-pituitary-adrenal axis in the mouse. *International Journal of Developmental Neuroscience* **21**:125–132. DOI: [https://doi.org/10.1016/s0736-5748\(03\)00030-3](https://doi.org/10.1016/s0736-5748(03)00030-3), PMID: 12711350
- Schmidt MV**. 2019. *Stress-Hyporesponsive Period*. CoLab. DOI: <https://doi.org/10.1016/B978-0-12-813146-6.00004-7>
- Seifert G**, Schilling K, Steinhäuser C. 2006. Astrocyte dysfunction in neurological disorders: a molecular perspective. *Nature Reviews. Neuroscience* **7**:194–206. DOI: <https://doi.org/10.1038/nrn1870>, PMID: 16495941
- Senst L**, Baimoukhametova D, Sterley TL, Bains JS. 2016. Sexually dimorphic neuronal responses to social isolation. *eLife* **5**:e18726. DOI: <https://doi.org/10.7554/eLife.18726>, PMID: 27725087

- Sharma SS**, Srinivas Bharath MM, Doreswamy Y, Laxmi TR. 2022. Effects of early life stress during stress hyporesponsive period (SHRP) on anxiety and curiosity in adolescent rats. *Experimental Brain Research* **240**:1127–1138. DOI: <https://doi.org/10.1007/s00221-022-06319-5>, PMID: 35141770
- Sun JD**, Liu Y, Yuan YH, Li J, Chen NH. 2012. Gap junction dysfunction in the prefrontal cortex induces depressive-like behaviors in rats. *Neuropsychopharmacology* **37**:1305–1320. DOI: <https://doi.org/10.1038/npp.2011.319>, PMID: 22189291
- Vázquez DM**. 1998. Stress and the developing limbic-hypothalamic-pituitary-adrenal axis. *Psychoneuroendocrinology* **23**:663–700. DOI: [https://doi.org/10.1016/s0306-4530\(98\)00029-8](https://doi.org/10.1016/s0306-4530(98)00029-8), PMID: 9854741
- Vivi E**, Di Benedetto B. 2024. Brain stars take the lead during critical periods of early postnatal brain development: relevance of astrocytes in health and mental disorders. *Molecular Psychiatry* **29**:2821–2833. DOI: <https://doi.org/10.1038/s41380-024-02534-4>, PMID: 38553540
- Wahis J**, Baudon A, Althammer F, Kerspern D, Goyon S, Hagiwara D, Lefevre A, Barteczko L, Boury-Jamot B, Bellanger B, Abatis M, Da Silva Gouveia M, Benusiglio D, Eliava M, Rozov A, Weinsanto I, Knobloch-Bollmann HS, Kirchner MK, Roy RK, Wang H, et al. 2021. Astrocytes mediate the effect of oxytocin in the central amygdala on neuronal activity and affective states in rodents. *Nature Neuroscience* **24**:529–541. DOI: <https://doi.org/10.1038/s41593-021-00800-0>, PMID: 33589833
- Walker C-D**, Bath KG, Joels M, Korosi A, Larauche M, Lucassen PJ, Morris MJ, Raineki C, Roth TL, Sullivan RM, Taché Y, Baram TZ. 2017. Chronic early life stress induced by limited bedding and nesting (LBN) material in rodents: critical considerations of methodology, outcomes and translational potential. *Stress* **20**:421–448. DOI: <https://doi.org/10.1080/10253890.2017.1343296>, PMID: 28617197
- Wamsteeker Cusulin JI**, Füzesi T, Inoue W, Bains JS. 2013. Glucocorticoid feedback uncovers retrograde opioid signaling at hypothalamic synapses. *Nature Neuroscience* **16**:596–604. DOI: <https://doi.org/10.1038/nn.3374>, PMID: 23563581
- Williamson MR**, Kwon W, Woo J, Ko Y, Maleki E, Yu K. 2024. Learning-associated astrocyte ensembles regulate memory recall. *Nature* **637**:478–486. DOI: <https://doi.org/10.1038/s41586-024-08170-w>
- Yu X**, Taylor A, Nagai J, Golshani P, Evans CJ, Coppola G, Khakh BS. 2018. Reducing astrocyte calcium signaling in vivo alters striatal microcircuits and causes repetitive behavior. *Neuron* **99**:1170–1187. DOI: <https://doi.org/10.1016/j.neuron.2018.08.015>, PMID: 30174118